The Onset of Thermal Runaway in Partially Insulated or Cooled Reactors

M. J. Ward
E. F. Van de Velde

CRPC-TR90062
July, 1990

Center for Research on Parallel Computation
Rice University
P.O. Box 1892
Houston, TX 77251-1892

1 Introduction

In steady state thermal explosion theory the dimensionless temperature distribution, u_0, in an exothermically active material is usually taken to satisfy a nonlinear elliptic equation of the form

$$\begin{aligned} \triangle u_0 + \lambda_0 F(x, u_0) = 0\,, \qquad & x \in D \\ \partial_n u_0 + b\, u_0 = 0\,, \qquad & x \in \partial D\,. \end{aligned} \tag{1.1}$$

Here the Biot number, b, and the two or three dimensional domain D are given and λ_0 is the Frank-Kamenetskii parameter. To model the reaction an Arrhenius heat generation term $F = \exp(u/(1+\beta u))$ is usually specified. The constant β is a dimensionless activation energy parameter with $\beta = 0$ corresponding to an infinite activation energy.

When F is taken to be the Arrhenius heating term, it is well known that, for some range of λ_0, multiple solutions can exist for (1.1). The conditions on b and β for the occurrence of these multiple solutions is also well established in some special geometries, (see Boddington et al. (1984) and the references therein for details). We now assume that, when multiple solutions to (1.1) occur, these solutions can be parameterized in terms of some parameter $\alpha > 0$, possibly the maximum temperature of the reactor, as $u_0(x,\alpha), \lambda_0(\alpha)$. The graph of α versus λ_0 is then multiple valued and has fold points at $\lambda_c = \lambda_0(\alpha_0)$ where $\lambda_0'(\alpha_0) = 0$ (see Fig. 2). The determination of these critical values of the Frank-Kamenetskii parameter is important in characterizing the thermal stability properties of the reactor. In particular, as λ_0 passes through λ_c a dramatic increase in the maximum temperature of the reactor can occur (see Fig. 2).

Of interest is to determine the effect upon λ_c of strong localized perturbations of (1.1). The first perturbation we treat is a deletion of a small subdomain D_ϵ from D with the imposition of a condition on the boundary of the resulting hole. The perturbed problem is

$$\triangle u + \lambda F(x,u) = 0\,, \qquad x \in D \backslash D_\epsilon \tag{1.2a}$$

$$\partial_n u + b\, u = 0\,, \qquad x \in \partial D \tag{1.2b}$$

$$\epsilon\, \partial_n u + \kappa\, u = 0\,, \qquad x \in \partial D_\epsilon\,. \tag{1.2c}$$

Here D_ϵ is a cooling rod or pellet of 'radius' ϵ, which is centered at some x_0 in D. The constant κ is the Biot number for the cooling rod or pellet and ∂_n denotes the outer normal to $D \backslash D_\epsilon$.

The second class of perturbations we examine is a large change in the constant b over a small part of the boundary. In this case the perturbed problem is

$$\Delta u + \lambda F(x,u) = 0\,, \qquad x \in D \tag{1.3a}$$

$$\partial_n u + b\,u = 0\,, \qquad x \in \partial D_0 \tag{1.3b}$$

$$\epsilon\,\partial_n u + \kappa\,u = 0\,, \qquad x \in \partial D_\epsilon\,, \tag{1.3c}$$

where $\partial D = \partial D_\epsilon \bigcup \partial D_0$. A schematic plot illustrating both classes of perturbations is shown in Fig 1 a,b.

Our goal here is to extend the asymptotic theory, initiated in Ward and Keller (1990), that was used to treat these two classes of strong localized perturbations of (1.1). We now give an outline of the present paper, highlighting our additional results for (1.2) and (1.3).

In §2 and §3 we review the theory presented in Ward and Keller (1990) for the determination of $\lambda_c(\epsilon)$, when $\epsilon \ll 1$, for both (1.2) and (1.3). These asymptotic results for $\lambda_c(\epsilon)$ are extended in §2 and §3 to ranges of b and κ not considered previously. In particular the case of almost total insulation, with $b = 0$ and $\kappa \neq 0$, is treated. The theory is presented allowing for an arbitrary heat generation term $F(x,u) > 0$ whereas for the examples in §4 and §5 we take F to be the Arrhenius heating term specified above.

In §4 we apply the asymptotic results of §2 to circular cylindrical and spherical reactors containing small cooling rods and pellets. The previous results of Ward and Keller (1990) are extended to the case of finite activation energies ($\beta > 0$) by using a numerical scheme to evaluate the coefficients in the asymptotic expansions of $\lambda_c(\epsilon)$. Additional results for the case of an almost totally insulated reactor are presented. The asymptotic results are compared with numerical solutions to (1.2) for special geometries, and clear agreement is obtained.

In §5 we apply the results of §3 to a slab reactor, in two dimensions, which has a small insulating segment of length 2ϵ on one side. This problem, with $\beta = 0$ was previously considered in Adler (1983), Greenway and Spence (1985), Herbert (1986), and Ward and

Keller (1990), where contradictory results for $\lambda_c(\epsilon)$ when $\epsilon \ll 1$ were obtained. To resolve this discrepancy, we first solve the two dimensional perturbed problem (1.3) numerically, using a high order difference method, on a finer mesh than that used in Greenway and Spence (1985). The numerical results for $\lambda_c(\epsilon)$ are then seen to strongly support the analytical predictions of Ward and Keller (1990). We also extend the results of Ward and Keller, for the slab reactor, to treat the case of finite activation energies where $\beta > 0$. These analytical predictions for $\lambda_c(\epsilon)$, for $\beta > 0$ and $\epsilon \ll 1$, are again seen to be in close agreement with numerical results for $\lambda_c(\epsilon)$ obtained from the numerical solution to (1.3).

Finally in §5 we also extend the analytical results of Ward and Keller (1990) to determine $\lambda_c(\epsilon)$, when $\beta \geq 0$ and $\epsilon \ll 1$, for other reactors with cooling or insulating patches on their boundaries.

2 Interior Perturbations: Theory

To solve (1.2) we write the solution in the parametric form $u(x, \alpha, \epsilon)$, $\lambda(\alpha, \epsilon)$, and we expand λ in terms of the unknown gauge functions $\nu_i(\epsilon)$ as

$$\lambda(\alpha, \epsilon) = \lambda_0(\alpha) + \nu_1(\epsilon)\lambda_1(\alpha) + \nu_2(\epsilon)\lambda_2(\alpha) + \cdots, \tag{2.1}$$

with $\nu_i(\epsilon) \ll 1$ and $\nu_{i+1}(\epsilon) = o[\nu_i(\epsilon)]$.

In the *outer region* away from D_ϵ we expand the solution as

$$u(x, \alpha, \epsilon) = u_0(x, \alpha) + \nu_1(\epsilon)u_1(x, \alpha) + \nu_2(\epsilon)u_2(x, \alpha) + \cdots. \tag{2.2}$$

Then substituting (2.1) and (2.2) in (1.2a, b) and collecting terms of order $\nu_1(\epsilon)$ we obtain

$$\begin{aligned} \Delta u_1 + \lambda_0 F_u(x, u_0)u_1 &= -\lambda_1 F(x, u_0), \qquad x \in D \backslash D_\epsilon \\ \partial_n u_1 + b\, u_1 &= 0, \qquad x \in \partial D\,. \end{aligned} \tag{2.3}$$

Equations for higher order corrections can be obtained in a similar manner.

In the *inner region* near D_ϵ we introduce the stretched variables $y = \epsilon^{-1}(x - x_0)$ and $v(y, \alpha, \epsilon) = u(x_0 + \epsilon y, \alpha, \epsilon)$. Then from (1.2$a, c$) we obtain

$$\begin{aligned} \Delta_y v + \epsilon^2\, \lambda\, F(x_0 + \epsilon y, v) &= 0, \qquad y \notin D_1 \\ \partial_n v + \kappa v &= 0, \qquad y \in \partial D_1\,. \end{aligned} \tag{2.4}$$

Here, ∂_n, Δ_y denote derivatives with respect to y, and D_1 is the domain D_ϵ in the y variable. Now we expand v in terms of the unknown gauge functions $\mu_i(\epsilon)$ as

$$v(y,\alpha,\epsilon) = \mu_0(\epsilon)v_0(y,\alpha) + \mu_1(\epsilon)v_1(y,\alpha) + \mu_2(\epsilon)v_2(y,\alpha) + \cdots . \tag{2.5}$$

Using (2.1) and (2.5) in (2.4), we obtain to leading order

$$\begin{aligned} \Delta_y v_0 &= 0, \qquad y \notin D_1 \\ \partial_n v_0 + \kappa v_0 &= 0, \qquad y \in \partial D_1 . \end{aligned} \tag{2.6}$$

Here we assumed that $\epsilon^2\lambda_0 F[x_0 + \epsilon y, \mu_0(\epsilon)v] = o[\mu_0(\epsilon)]$. Equations for v_1, v_2, etc. can be obtained in the same way.

The two expansions (2.2) and (2.5) must be asymptotically equal to one another in an overlap domain where $x - x_0$ is small and $y = \epsilon^{-1}(x - x_0)$ is large. Upon expanding u_0 in powers of $x - x_0$ we can write this matching condition as

$$\begin{aligned} u_0(x_0) + (x_i - x_{0i})\,\partial_{x_i} u_0(x_0) + \frac{1}{2}(x_i - x_{0i})\,\partial_{x_i}\partial_{x_j} u_0(x_0)(x_j - x_{0j}) + \nu_1(\epsilon)u_1(x) + \cdots \\ \sim \mu_0(\epsilon)v_0(y) + \mu_1(\epsilon)v_1(y) + \mu_2(\epsilon)v_2(y) + \cdots . \end{aligned} \tag{2.7}$$

To continue further we must determine the asymptotic behavior of u_1, u_2, etc. for x near x_0 and of v_0, v_1 for $|y| \to \infty$, which we do in §2.1 and §2.2 .

To determine the perturbation in the location of the fold point we solve $\lambda_\alpha(\alpha,\epsilon) = 0$ for $\alpha(\epsilon)$, which is expanded as $\alpha(\epsilon) = \alpha_0 + \nu_1(\epsilon)\alpha_1 + \cdots$. Using this expansion and (2.1) in $\lambda_\alpha = 0$ we find $\alpha_1 = -\lambda_1'(\alpha_0)/\lambda_0''(\alpha_0)$ so that

$$\lambda_c \equiv \lambda[\alpha_0 + \nu_1(\epsilon)\alpha_1 + \cdots, \epsilon] = \lambda_0(\alpha_0) + \nu_1(\epsilon)\lambda_1(\alpha_0) + \cdots , \tag{2.8}$$

which to this order is independent of α_1.

To determine $\lambda_1(\alpha_0)$ we first differentiate (1.1) with respect to α to obtain

$$\begin{aligned} \Delta u_{0\alpha} + \lambda_0 F_u(x,u_0)u_{0\alpha} &= -\lambda_0'\,F(x,u_0), \qquad x \in D \\ \partial_n u_{0\alpha} + b\,u_{0\alpha} &= 0, \qquad x \in \partial D . \end{aligned} \tag{2.9}$$

At the fold point $\alpha = \alpha_0$ we have $\lambda_0'(\alpha_0) = 0$ by assumption, so (2.9) is the homogeneous form of (2.3). Assuming that the operator in (2.3) has a one-dimensional nullspace at α_0

then the inhomogeneous term in (2.3) must satisfy one solvability condition. To derive that condition we apply Green's theorem to $u_{0\alpha}$ and u_1 in the domain $D\backslash D_\rho$ where D_ρ is a small sphere or circle of radius ρ centered at x_0. Then we let $\rho \to 0$ to obtain at $\alpha = \alpha_0$

$$\lambda_1(\alpha_0) = -\frac{\lim_{\rho\to 0}\int_{\partial D_\rho}(u_{0\alpha}\partial_n u_1 - u_1\partial_n u_{0\alpha})\,ds}{\int_D u_{0\alpha}F(x,u_0)\,dx}\,. \tag{2.10}$$

This equation determines $\lambda_1(\alpha_0)$ in terms of the behavior of u_1 near x_0, which is determined below. Thus the leading order perturbation in λ_c is just $\nu_1(\epsilon)\lambda_1(\alpha_0)$ where $\lambda_1(\alpha_0)$ is given by (2.10).

2.1 The Three Dimensional Case

In three dimensions (2.6) has a unique solution, which tends to $u_0(x_0)$ at infinity. Its asymptotic form is

$$v_0(y) \sim u_0(x_0)\Big[1 - \frac{C(\kappa)}{|y|} + \cdots\Big] \quad \text{as } |y| \to \infty\,. \tag{2.11}$$

With $\mu_0(\epsilon) = 1$ the leading terms in (2.7) match, and the $\nu_1(\epsilon)u_1(x)$ term must then match the singular term $-u_0(x_0)C(\kappa)/|y|$. Thus we must have that

$$\nu_1(\epsilon) = \epsilon, \qquad u_1(x) \sim -u_0(x_0)\frac{C(\kappa)}{|x-x_0|} \quad \text{as} \quad x \to x_0\,. \tag{2.12}$$

Using this asymptotic behavior for u_1 in (2.10) we find

$$\lambda_1(\alpha_0) = \frac{4\pi\, C(\kappa)\, u_0(x_0,\alpha_0)\, u_{0\alpha}(x_0,\alpha_0)}{\int_D u_{0\alpha}(x,\alpha_0)F[x,u_0(x,\alpha_0)]\,dx}\,, \tag{2.13a}$$

and from (2.8) we have

$$\lambda_c = \lambda_0(\alpha_0) + \epsilon\,\lambda_1(\alpha_0) + \cdots, \qquad b \neq 0\,. \tag{2.13b}$$

In the case where $\kappa = \infty$, then $C(\infty)$ is the capacitance of D_1. Alternatively when $\kappa = 0$ then $C(0) = 0$ so (2.13a,b) gives no correction at this order.

To determine the first nonvanishing correction to the fold point when $\kappa = 0$ we must retain higher order correction terms in the inner region. Noting that $v_0 = u_0(x_0)$ in this

case, we choose $\mu_1(\epsilon) = \epsilon$ and $\mu_2(\epsilon) = \epsilon^2$ in (2.5) to match to the second and third terms on the left side of (2.7). Then from (2.4) we obtain, for $y \notin D_1$,

$$\begin{aligned} &\triangle_y v_1 = 0\,; \quad \partial_n v_1 = 0, \ y \in \partial D_1 \qquad v_1(y) \sim y_i\, \partial_{x_i} u_0(x_0) \quad \text{as } y \to \infty\,, \\ &\triangle_y v_2 = -\lambda_0 F(x_0, v_0)\,; \quad \partial_n v_2 = 0\,, \ y \in \partial D_1 \quad v_2(y) \sim \frac{1}{2} y_i\, y_j\, \partial_{x_i}\partial_{x_j} u_0(x_0) \quad \text{as } y \to \infty\,. \end{aligned} \tag{2.14}$$

The asymptotic behavior of v_1 and v_2 is given by (see Ward and Keller (1990))

$$v_1(y) \sim \partial_{x_i} u_0(x_0)\Big[y_i + \frac{P_{ij} y_j}{|y|^3} + \cdots\Big] \qquad v_2(y) \sim \frac{1}{2} y_i\, y_j\, \partial_{x_i}\partial_{x_j} u_0(x_0) - \frac{B(\alpha)}{|y|}\,, \tag{2.15}$$

as $y \to \infty$. Here P_{ij} is the polarizability tensor of D_1 and

$$B(\alpha) = \frac{\lambda_0(\alpha)}{4\pi} V_1\, F[x_0, u_0(x_0, \alpha)]\,, \tag{2.16}$$

where V_1 is the volume of D_1. Rewriting (2.15) in outer variables and matching to the fourth term on the left side of (2.7) we have that

$$\nu_1(\epsilon) = \epsilon^3\,, \qquad u_1 \sim \partial_{x_i} u_0(x_0, \alpha)\, \frac{P_{ij}(x_j - x_{0j})}{|x - x_0|^3} - \frac{B(\alpha)}{|x - x_0|} \qquad \text{as } x \to x_0\,.$$

From (2.10) we find at $\alpha = \alpha_0$ that

$$\lambda_1(\alpha_0) = 4\pi \frac{B(\alpha_0) u_{0\alpha}(x_0, \alpha_0) - \partial_{x_i} u_{0\alpha}(x_0, \alpha_0)\, P_{ij}\, \partial_{x_j} u_0(x_0, \alpha_0)}{\int_D u_{0\alpha}(x, \alpha_0) F[x, u_0(x, \alpha_0)]\, dx}\,, \tag{2.17a}$$

where $B(\alpha)$ is given in (2.16). Finally (2.8) yields

$$\lambda_c = \lambda_0(\alpha_0) + \epsilon^3 \lambda_1(\alpha_0) + \cdots \quad \text{when } \kappa = 0\,, \quad b \neq 0\,. \tag{2.17b}$$

Now we extend the results of Ward and Keller (1990) to treat the case where $\kappa = \epsilon\kappa_0$, with $\kappa_0 = O(1)$, so that $\partial_n u + \kappa_0 u = 0$ on the boundary of the hole. In this case we expand $v = u_0(x_0) + \epsilon v_1 + \cdots$ so that from (2.4), v_1 satisfies

$$\triangle_y v_1 = 0\,, \quad \partial_n v_1 = -\kappa_0 u_0(x_0)\,, \ y \in \partial D_1 \qquad v_1(y) \sim y_i\, \partial_{x_i} u_0(x_0) \quad \text{as } y \to \infty\,. \tag{2.18a}$$

The asymptotic behavior of v_1 now includes a monopole term, and using the divergence theorem we find

$$v_1(y) \sim \partial_{x_i} u_0(x_0) y_i - \frac{S_1\, u_0(x_0)\, \kappa_0}{4\,\pi\,|y|} + O(|y|^{-2})\,.$$

Here, S_1 is the surface area of ∂D_1. Matching to the fourth term on the left side of (2.7) we have that

$$\nu_1(\epsilon) = \epsilon^2\,, \qquad u_1 \sim -\frac{S_1\, u_0(x_0)\,\kappa_0}{4\,\pi\,|x-x_0|} \qquad \text{as } x \to x_0\,.$$

From (2.10) we find at $\alpha = \alpha_0$ that

$$\lambda_c = \lambda_0(\alpha_0) + \epsilon^2\lambda_1(\alpha_0) + \cdots \qquad \lambda_1(\alpha_0) = \frac{S_1\,\kappa_0\,u_0(x_0,\alpha_0)\,u_{0\alpha}(x_0,\alpha_0)}{\int_D u_{0\alpha}(x,\alpha_0)F[x,u_0(x,\alpha_0)]\,dx}\,, \qquad (2.18b)$$

when $\kappa = \epsilon\kappa_0$ and $b \neq 0$.

We also extend the results of Ward and Keller (1990) to treat the case where the outer boundary is perfectly insulating, $b = 0$, and on the inner boundary $\kappa \neq 0$ and $\kappa = O(1)$. For simplicity, we assume below that F is independent of x so that $F(x,u) = F(u) > 0$.

When $b = 0$, solutions to (1.1) exist only if $\lambda_0 = 0$. If $\lambda_0 = 0$, the solutions to (1.1) are arbitrary constants, and we label $u_0(x,\alpha) = \alpha$. Since the inhomogeneous term in (2.3) must satisfy one solvability condition at each α, (2.10) still holds with α_0 replaced by α. Setting $u_0(x,\alpha) = \alpha$ in (2.13a) and assuming that F is uniform in x, we derive that

$$\lambda(\alpha) = \epsilon\,\lambda_1(\alpha) + \cdots\,, \qquad \text{with} \qquad \lambda_1(\alpha) = \frac{4\,\pi\,C(\kappa)\,\alpha}{V\,F(\alpha)}\,. \qquad (2.19)$$

Here, V is the volume of D. The location of the fold points are given by $\lambda(\alpha_0)$ where $\lambda_1'(\alpha_0) = 0$.

2.2 The Two Dimensional Case

In two dimensions (2.6) has a solution which has the asymptotic form

$$v_0(y) = u_0(x_0)\left(\log|y| + d(\kappa) + \cdots\right) \quad \text{as} \quad |y| \to \infty, \quad \kappa \neq 0\,. \qquad (2.20)$$

If $\kappa \neq 0$ the constant $d(\kappa)$ is uniquely determined, whereas if $\kappa = 0$ then $d(0)$ is arbitrary.

We first consider the case $\kappa \neq 0$. To match the leading terms in (2.7), we must take $\mu_0(\epsilon) = -1/\log\epsilon$. Then, to match the fourth term on the left side of (2.7) we require that

$$\nu_1(\epsilon) = -1/\log\epsilon\,, \qquad u_1 \sim u_0(x_0)[\log|x-x_0| + d(\kappa)] \qquad \text{as } x \to x_0\,. \qquad (2.21)$$

Using (2.21) in (2.10) we obtain that

$$\lambda_1(\alpha_0) = \frac{2\pi\,u_0(x_0,\alpha_0)\,u_{0\alpha}(x_0,\alpha_0)}{\int_D u_{0\alpha}(x,\alpha_0)F[x,u_0(x,\alpha_0)]\,dx}\,, \qquad (2.22a)$$

and from (2.8) we have that

$$\lambda_c = \lambda_0(\alpha_0) - \frac{1}{\log \epsilon}\lambda_1(\alpha_0) + \cdots \qquad \text{when} \quad \kappa \neq 0\,, \quad b \neq 0\,. \tag{2.22b}$$

In the special case $\kappa = 0$, we take $v_0(y) = u_0(x_0)$, $\mu_1(\epsilon) = \epsilon$, and $\mu_2(\epsilon) = \epsilon^2$ in (2.5), and derive (2.14). The asymptotic behavior of v_1 and v_2 as $y \to \infty$, analogous to (2.15), is given by

$$v_1(y) \sim \partial_{x_i} u_0(x_0)\Big[y_i + \frac{P_{ij}y_j}{|y|^2} + \cdots\Big] \qquad v_2(y) \sim \frac{1}{2} y_i\, y_j\, \partial_{x_i}\partial_{x_j} u_0(x_0) + B(\alpha)\log|y|\,, \tag{2.23}$$

where

$$B(\alpha) = \frac{\lambda_0(\alpha)\, A_1}{2\pi} F[x_0, u_0(x_0,\alpha)]\,. \tag{2.24}$$

Here A_1 is the area of D_1. From the matching condition (2.7) we require that

$$\nu_1(\epsilon) = \epsilon^2, \qquad u_1 \sim \partial_{x_i} u_0(x_0,\alpha)\,\frac{P_{ij}(x_j - x_{0j})}{|x - x_0|^2} + B(\alpha)\log|x - x_0| \quad \text{as} \quad x \to x_0\,.$$

Using the solvability condition (2.10) we obtain that

$$\lambda_1(\alpha_0) = 2\pi \frac{B(\alpha_0) u_{0\alpha}(x_0,\alpha_0) - \partial_{x_i} u_{0\alpha}(x_0,\alpha_0)\, P_{ij}\, \partial_{x_j} u_0(x_0,\alpha_0)}{\int_D u_{0\alpha}(x,\alpha_0) F[x, u_0(x,\alpha_0)]\, dx}\,, \tag{2.25a}$$

and the correction to the fold point from (2.8) is

$$\lambda_c = \lambda_0(\alpha_0) + \epsilon^2\lambda_1(\alpha_0) + \cdots \qquad \text{when} \quad \kappa = 0\,, \quad b \neq 0\,. \tag{2.25b}$$

We now treat the case where $\kappa = \epsilon\kappa_0$ with $\kappa_0 = O(1)$. In the inner region we expand $v = u_0(x_0) + \epsilon v_1 + \cdots$ to derive (2.18a). Then, using the divergence theorem, the far field behavior of the inner solution is

$$v_1(y) \sim \partial_{x_i} u_0(x_0) y_i + \frac{L_1\, u_0(x_0)\,\kappa_0}{2\,\pi}\log|y| + \cdots\,. \tag{2.26a}$$

Here, L_1 is the length of ∂D_1. Matching to the fourth term on the left side of (2.7) we find that

$$\nu_1(\epsilon) = \epsilon\,, \qquad u_1 \sim \frac{L_1\, u_0(x_0)\,\kappa_0}{2\,\pi}\log|x - x_0| \qquad \text{as} \quad x \to x_0\,.$$

From (2.10) we find at $\alpha = \alpha_0$ that

$$\lambda_c = \lambda_0(\alpha_0) + \epsilon\lambda_1(\alpha_0) + \cdots \qquad \lambda_1(\alpha_0) = \frac{L_1\,\kappa_0\,u_0(x_0,\alpha_0)\,u_{0\alpha}(x_0,\alpha_0)}{\int_D u_{0\alpha}(x,\alpha_0)F[x,u_0(x,\alpha_0)]\,dx}\,, \qquad (2.26b)$$

when $\kappa = \epsilon\kappa_0$ and $b \neq 0$. We remark that in the matching we had to insert a term $(\epsilon \log \epsilon)\hat{v}$ in the inner expansion. Since $\hat{v}$ satisfies Laplace's equation with $\partial_n\hat{v} = 0$ on D_1, we take $\hat{v} = \kappa_0\,L_1\,u_0(x_0)/(2\pi)$ to cancel the unmatched term from the inner expansion.

Finally, we treat the case where the outer boundary is perfectly insulating, $b = 0$, and we proceed as in §2.1. Assuming $F(x,u) = F(u) > 0$ and labeling $u_0(x,\alpha) = \alpha$, we derive, analogous to (2.19), that

$$\lambda(\alpha) = (\frac{-1}{\log\epsilon})\,\lambda_1(\alpha) + \cdots\,, \quad \text{with} \qquad \lambda_1(\alpha) = \frac{2\,\pi\,\alpha}{A\,F(\alpha)}\,. \qquad (2.27)$$

Here, A is the area of D. The location of the fold point is again found by setting $\lambda_1'(\alpha) = 0$.

3 Boundary Perturbations: Theory

To treat (1.3) we proceed by the method of §2. The equations of §2 still apply with two modifications. First, the domain within which the inner problems are to be solved is the half-space bounded by the tangent plane (3-D) or tangent line (2-D) to ∂D at x_0. In addition, in (2.10) ∂D_ρ denotes only that part of ∂D_ρ lying in D and that part tends to a hemisphere (3-D) or a semi-circle (2-D) as ρ tends to zero.

3.1 The Two Dimensional Case

In the neighborhood of x_0, we introduce orthogonal curvilinear coordinates (s,n) with origin at x_0, where s measures arclength along ∂D and $-n$ is the distance from x to ∂D. From (1.3) we find that

$$\begin{aligned} u_{nn} + \frac{1}{p+n}u_n + \frac{1}{(1+p^{-1}n)^2}u_{ss} + \lambda\,F(x,u) = 0, \qquad & x \in D \\ \partial_n u + b\,u = 0, \quad \text{on } n = 0\,, \qquad & |s| > \epsilon\,, \\ \epsilon\,\partial_n u + \kappa\,u = 0, \quad \text{on } n = 0\,, \qquad & |s| < \epsilon\,, \end{aligned} \qquad (3.1)$$

where p is the radius of curvature of ∂D.

In the *inner region* we introduce $\xi = \epsilon^{-1}s$, $\eta = \epsilon^{-1}n$ and $v(\xi,\eta,\epsilon) = u(s,n,\epsilon)$ and we expand $v = \mu_0(\epsilon)v_0 + \mu_1(\epsilon)v_1 + \cdots$. From (3.1), we obtain to leading order

$$\begin{aligned} &v_{0\xi\xi} + v_{0\eta\eta} = 0\,, \quad \eta < 0 \\ &\qquad \partial_\eta v_0 = 0 \quad (b < \infty) \quad \text{or} \quad v_0 = 0 \quad (b = \infty)\,, \quad \eta = 0\,, \quad |\xi| > 1 \\ &\partial_\eta v_0 + k v_0 = 0\,, \quad \eta = 0\,, \quad |\xi| < 1\,. \end{aligned} \tag{3.2}$$

To determine $\lambda_1(\alpha_0)$ we use the matching condition (2.7) where the left side of (2.7) is replaced by

$$u(s,n,\epsilon) \sim u_0(0,0) + n\,\partial_n u_0(0,0) + s\,\partial_s u_0(0,0) + \nu_1(\epsilon)u_1(s,n) + \cdots\,. \tag{3.3}$$

We now determine the correction to the fold point for four different ranges of b and κ.

If $0 < b < \infty$ and $\kappa \neq 0$ then in general $u_0(0,0) \neq 0$. In this case (3.2) has a solution which has the asymptotic form

$$v_0(y) = u_0(0,0)\left(\log|y| + d(\kappa) + \cdots\right) \quad \text{as} \quad |y| = (\xi^2+\eta^2)^{1/2} \to \infty.$$

The leading terms in (2.7) are matched with $\mu_0(\epsilon) = -1/\log\epsilon$, and to match the fourth term on the left side of (3.3) we require that

$$\nu_1(\epsilon) = -1/\log\epsilon\,, \qquad u_1(s,n) \sim u_0(0,0)\left(\frac{1}{2}\log(n^2+s^2) + d(\kappa)\right) \tag{3.4}$$

as $(n^2+s^2)^{1/2} \to 0$. Using (3.4) in (2.10) and (2.8) we obtain that

$$\lambda_c = \lambda_0(\alpha_0) - \frac{1}{\log\epsilon}\lambda_1(\alpha_0) + \cdots\,, \qquad \lambda_1(\alpha_0) = \frac{\pi u_0(x_0,\alpha_0)\,u_{0\alpha}(x_0,\alpha_0)}{\int_D u_{0\alpha}(x,\alpha_0)F[x,u_0(x,\alpha_0)]\,dx}\,, \tag{3.5}$$

when $0 < b < \infty$ and $\kappa \neq 0$.

If $b = \infty$ and $\kappa \neq \infty$ then $u_0(0,0) = 0$ and $\partial_s u_0(0,0) = 0$. In this case, we take $\mu_0(\epsilon) = \epsilon$ and require that $v_0(\xi,\eta) \sim \eta\partial_n u_0(0,0)$ as $\eta \to -\infty$. Then there is a solution to (3.2) which has the asymptotic form given by

$$v_0(\xi,\eta) = \partial_n u_0(0,0)\Big[\eta + \frac{e(\kappa)\,\eta}{\xi^2+\eta^2} + \cdots\Big]\,, \quad \xi^2+\eta^2 \gg 1\,,$$

for some $e(\kappa)$. Thus matching v_0 to the term $\nu_1(\epsilon)u_1$ in (3.3), we obtain that

$$\nu_1(\epsilon) = \epsilon^2\,, \qquad u_1(s,n) \sim \partial_n u_0(0,0)\frac{e(\kappa)\,\eta}{n^2+s^2} \quad \text{as} \quad n^2+s^2 \to 0\,. \tag{3.6}$$

Using (3.6) in (2.10) and (2.8) the correction to the fold point is

$$\lambda_c = \lambda_0(\alpha_0) + \epsilon^2\lambda_1(\alpha_0) + \cdots, \qquad \lambda_1(\alpha_0) = -\frac{\pi\, e(\kappa)\, \partial_n u_{0\alpha}(x_0,\alpha_0)\, \partial_n u_0(x_0,\alpha_0)}{\int_D u_{0\alpha}(x,\alpha_0) F[x,u_0(x,\alpha_0)]\, dx}, \quad (3.7)$$

when $b = \infty$ and $\kappa \neq \infty$. When $\kappa = 0$ then an explicit solution to (3.2) can be found and we obtain $e(0) = 1/2$.

We now analyze two additional cases not considered in Ward and Keller (1990). First, we assume that the Biot number changes by an $O(1)$ amount near the cooling segment so that $b < \infty$ and $\kappa = \epsilon\kappa_0$. Then it is shown below that the correction to the fold point is proportional to $b - \kappa_0$. Secondly, we will treat the case of an almost totally insulated boundary so that $b = 0$ and $\kappa \neq 0$.

If $0 < b < \infty$ and $\kappa = \epsilon\kappa_0$ then in general $u_0(0,0) \neq 0$. In this case we take $\mu_0(\epsilon) = 1$ and $\mu_1(\epsilon) = \epsilon$ and we expand $v = u_0(0,0) + \epsilon v_1 + \cdots$. Then from (3.1), v_1 solves

$$\begin{aligned} &v_{1\xi\xi} + v_{1\eta\eta} = 0, \quad \eta < 0 \\ &\partial_\eta v_1 = -b\, u_0(0,0) \quad \xi > 1, \qquad \partial_\eta v_1 = -\kappa_0\, u_0(0,0) \quad \xi < 1, \qquad \text{on } \eta = 0. \end{aligned} \quad (3.8)$$

Using the divergence theorem it can easily be shown that there is a solution to (3.8) with the following asymptotic form

$$v_1(\xi,\eta) \sim -b\eta\, u_0(0,0) - \frac{2}{\pi}(b-\kappa_0)\, u_0(0,0) \log((\xi^2+\eta^2)^{1/2}) + \xi\, \partial_s u_0(0,0) + \cdots. \quad (3.9)$$

Writing (3.9) in outer variables and noting that $\partial_n u_0(0,0) + b u_0(0,0) = 0$, then the far field behavior of the inner solution $v = u_0(0,0) + \epsilon v_1 + \cdots$ is given by

$$v \sim u_0(0,0) + n\, \partial_n u_0(0,0) + s\, \partial_s u_0(0,0) + \frac{2\epsilon}{\pi}(b-\kappa_0) u_0(0,0)\big(\log\epsilon - \log[(\xi^2+\eta^2)^{1/2}]\big) + \cdots. \quad (3.10)$$

Comparing (3.10) with (3.3) we must take

$$\nu_1(\epsilon) = \epsilon, \qquad u_1(s,n) \sim -\frac{2}{\pi}(b-\kappa_0) u_0(0,0)\, \log((n^2+s^2)^{1/2}) \quad \text{as } (n^2+s^2)^{1/2} \to 0. \quad (3.11)$$

The term of order $\epsilon\log\epsilon$ in (3.10) is unmatched thus far, which shows that we must include a term $(\epsilon\log\epsilon)\hat{v}(y)$ in the inner expansion. Since $\hat{v}$ satisfies Laplace's equation with $\partial_n\hat{v} = 0$

on $\eta = 0$, we can take $\hat{v} = -2(b - \kappa_0)u_0(0,0)/\pi$ to cancel exactly the unmatched term in (3.10). Finally, using (3.11) in (2.10) and (2.8) the correction to the fold point is

$$\lambda_c = \lambda_0(\alpha_0) + \epsilon\lambda_1(\alpha_0) + \cdots, \qquad \lambda_1(\alpha_0) = \frac{2(\kappa_0 - b)u_0(x_0,\alpha_0)\, u_{0\alpha}(x_0,\alpha_0)}{\int_D u_{0\alpha}(x,\alpha_0)F[x,u_0(x,\alpha_0)]\,dx}, \tag{3.12}$$

when $b < \infty$ and $\kappa = \epsilon\kappa_0$.

When $b = 0$ and $\kappa \neq 0$, the boundary is almost totally insulated. Assuming F is uniform in x so that $F(x,u) = F(u) > 0$, we proceed as in §2.2 to derive (2.27) with 2π replaced by π. Thus

$$\lambda(\alpha) = (-1/\log\epsilon)\lambda_1(\alpha) + \cdots \quad \text{with} \qquad \lambda_1(\alpha) = \frac{\pi\,\alpha}{A\,F(\alpha)}. \tag{3.13}$$

Here, A is the area of D and the location of the possible fold points are at $\lambda(\alpha_0)$ where $\lambda_1'(\alpha_0) = 0$.

3.2 The Three Dimensional Case

The procedure followed in the two-dimensional case can be adapted to treat the three-dimensional case. Since the analysis is similar to that in §3.1 we shall omit the details. Below we give expressions for the fold point corrections for the four ranges of b and κ that were considered in §3.1.

If $0 < b < \infty$ and $\kappa \neq 0$, the correction to the fold point is given by

$$\lambda_c = \lambda_0(\alpha_0) + \epsilon\,\lambda_1(\alpha_0) + \cdots, \qquad \lambda_1(\alpha_0) = \frac{2\pi\, C(\kappa)\, u_0(x_0,\alpha_0)\, u_{0\alpha}(x_0,\alpha_0)}{\int_D u_{0\alpha}(x,\alpha_0)F[x,u_0(x,\alpha_0)]\,dx}. \tag{3.14}$$

The constant $C(\kappa)$ is determined from the following canonical problem:

$$\begin{aligned} &v_{\xi_1\xi_1} + v_{\xi_2\xi_2} + v_{\eta\eta} = 0\,, \quad \eta < 0 \\ &\partial_\eta v = 0 \quad (\xi_1,\xi_2) \notin \partial D_1\,, \quad \partial_\eta v + \kappa v = 0 \quad (\xi_1,\xi_2) \in \partial D_1\,, \quad \text{on } \eta = 0\,, \\ &v \sim 1 - C(\kappa)/|y| + \cdots \qquad \text{as } |y| = (\xi_1^2 + \xi_2^2 + \eta^2)^{1/2} \to \infty\,. \end{aligned} \tag{3.15}$$

Here ∂D_1 denotes the perturbing patch ∂D_ϵ magnified by ϵ^{-1}. If ∂D_1 is a circular patch of radius one and $\kappa = \infty$ then $C(\infty) = 2/\pi$ is the well-known result for the capacitance of a charged circular disk.

If $b = \infty$ and $\kappa \neq \infty$, the correction to the fold point is given by

$$\lambda_c = \lambda_0(\alpha_0) + \epsilon^3 \lambda_1(\alpha_0) + \cdots, \qquad \lambda_1(\alpha_0) = -\frac{2\pi e(\kappa)\, \partial_n u_{0\alpha}(x_0, \alpha_0)\, \partial_n u_0(x_0, \alpha_0)}{\int_D u_{0\alpha}(x, \alpha_0) F[x, u_0(x, \alpha_0)]\, dx}. \quad (3.16)$$

Here, the constant $e(\kappa)$, representing one element of the polarizability tensor, is determined from the following canonical problem:

$$\begin{aligned} & v_{\xi_1\xi_1} + v_{\xi_2\xi_2} + v_{\eta\eta} = 0, \quad \eta < 0 \\ & v = 0 \quad (\xi_1, \xi_2) \notin \partial D_1, \quad \partial_\eta v + \kappa v = 0 \quad (\xi_1, \xi_2) \in \partial D_1, \quad \text{on } \eta = 0, \\ & v \sim \eta + \frac{e(\kappa)\,\eta}{|y|^3} + \cdots \quad \text{as} \quad |y| = (\xi_1^2 + \xi_2^2 + \eta^2)^{1/2} \to \infty. \end{aligned} \quad (3.17)$$

If ∂D_1 is a circular patch of radius one and $\kappa = 0$, then an explicit solution to (3.17) provides $e(0) = 2/3\pi$.

If $0 < b < \infty$ and $\kappa = \epsilon \kappa_0$, the correction to the fold point is given by

$$\lambda_c = \lambda_0(\alpha_0) + \epsilon^2 \lambda_1(\alpha_0) + \cdots, \qquad \lambda_1(\alpha_0) = \frac{A_1(\kappa_0 - b)\, u_0(x_0, \alpha_0)\, u_{0\alpha}(x_0, \alpha_0)}{\int_D u_{0\alpha}(x, \alpha_0) F[x, u_0(x, \alpha_0)]\, dx}, \quad (3.18)$$

where A_1 is the area of the scaled patch ∂D_1.

Finally, when the boundary is almost totally insulated with $b = 0$ and $\kappa \neq 0$ then, upon assuming $F(x, u) = F(u) > 0$, we find that

$$\lambda(\alpha) = \epsilon \lambda_1(\alpha) + \cdots \quad \text{with} \qquad \lambda_1(\alpha) = \frac{2\pi\, \alpha\, C(\kappa)}{V\, F(\alpha)}. \quad (3.19)$$

Here V is the volume of D and $C(\kappa)$ is determined from (3.15). The possible fold points are again found by setting $\lambda_1'(\alpha) = 0$.

4 Interior Perturbations: Comparison of Asymptotics and Numerics

We now apply the results of §2 to determine the effect of a small cooling pellet or rod on a model chemical reactor. To model our reactor, we take the Arrhenius heat generation term with finite activation energy so that $F(x, u) = F(u, \beta) \equiv \exp(u/(1 + \beta u))$, where $\beta \geq 0$. We now briefly review some well-known results on the qualitative behavior of solutions to the unperturbed problem (1.1), with the Arrhenius heating term specified above, in circular or spherical domains. A detailed discussion and proof of some of these results can be found in Bebernes and Eberly (1989) and the references therein.

All positive solutions to (1.1) in circular or spherical domains are radially symmetric and are monotone decreasing functions of $r = |x|$ for $r > 0$. If $\beta = 0$ and $0 < b \leq \infty$, there exists some $\lambda_c < \infty$ such that there is no solution to (1.1) for all $\lambda > \lambda_c$. If $\lambda < \lambda_c$, and $0 < b \leq \infty$, there are two solutions to (1.1) in the two-dimensional case. In three dimensions, the case $\beta = 0$ is somewhat more complicated. In this case, if $b = \infty$ there exists a λ_m such that (1.1) has a countable infinity of solutions if $\lambda = \lambda_m$. In addition, if $\lambda \in (0, \lambda_c)$ and $\lambda \neq \lambda_m$ then there is a finite number of solutions to (1.1).

If $\beta > 0$ and $0 < b \leq \infty$, then solutions to (1.1) exist for all $\lambda \geq 0$ in both the two and three dimensional cases. Furthermore, if $\beta \geq \beta_c(b)$, the solutions to (1.1) are unique for all $\lambda \geq 0$. However, when $\beta < \beta_c(b)$, multiple steady state solutions occur for some range of λ. This critical value of β, labeled by $\beta_c(b)$, has been computed numerically in Boddington et al. (1983) for various values of b in both the two and three dimensional cases. A schematic plot of the maximum temperature versus λ, which illustrates the possible solution multiplicity in the two dimensional case for $\beta = 0$ and $\beta \neq 0$, is shown in Fig. 2. Finally, we mention that explicit formulas for the solutions to (1.1) can only be found in the two dimensional case when $\beta = 0$.

We now describe our computational schemes to treat cylindrical and spherical reactors with small cooling rods or pellets when $\beta \geq 0$. For simplicity we assume that the reactor has radius one, and for the moment we take the location of the cooling rod or pellet to be at $r_0 \in [0, 1)$.

The Computational Schemes

To determine the asymptotic results for the fold corrections in various cases, a computational scheme to evaluate $\lambda_1(\alpha_0)$, given in (2.13a), (2.17a), (2.22a) and (2.25a), is needed. We now present such a scheme for spherical and circular cylindrical domains in which the unperturbed solution $u_0(r)$ satisfies a boundary value problem for ordinary differential equations. We begin by considering the extended system obtained from (1.1) and (2.9) in the domain $r = |x| \leq 1$, which is written as,

$$u_0'' + \frac{(m-1)}{r} u_0' + \lambda_0 F(u_0, \beta) = 0\,, \qquad F(u, \beta) = \exp\left(u/(1+\beta u)\right), \qquad (4.1a)$$

$$u''_{0\alpha} + \frac{(m-1)}{r} u'_{0\alpha} + \lambda_0 F_u(u_0, \beta) = \lambda'_0 F(u_0, \beta), \tag{4.1b}$$

$$u'_0 + b u_0 = 0, \qquad u'_{0\alpha} + b u_{0\alpha} = 0 \quad \text{on } r = 1, \quad b \neq 0 \tag{4.1c}$$

$$u'_0(0) = 0, \quad u'_{0\alpha}(0) = 0, \quad u_0(0) = \alpha, \quad u_{0\alpha}(0) = 1. \tag{4.1d}$$

Here α is chosen to be the maximum temperature for the unperturbed problem, and m is the number of spatial dimensions.

To determine the location of the 'first' fold point (see Fig. 2) for the unperturbed problem for fixed β, we solve (4.1) subject to the side condition $\lambda'_0(\alpha_0) = 0$ and $\lambda'_0(\alpha) > 0$ for $0 < \alpha < \alpha_0$. For fixed α and β the boundary value problem (4.1) is solved for u_0, $u_{0\alpha}$, λ_0, and λ'_0 using the collocation package COLSYS developed by Ascher et al. (1979). A simple continuation in α, starting from $\alpha \approx .05$, is used to determine the first sign change of λ'_0. Then, a Newton iteration scheme is employed to locate the first fold point $(\lambda_0(\alpha_0), \alpha_0)$ accurately. Once this fold point is located accurately the quantities $u_0(r_0)$, $u_{0\alpha}(r_0)$ etc..., which are needed for the computation of the fold point correction $\lambda_1(\alpha_0)$ in (2.13a), (2.17a) and (2.22a), (2.25a), are available. The integral appearing in these expressions for the fold point correction is evaluated at $\alpha = \alpha_0$ using Simpson's rule. In the special case $\beta = 0$ this integral can be evaluated analytically using (2.9) and the divergence theorem. Finally, a simple continuation scheme in β, using the previous solution as an initial guess, is used to locate the first fold point, and hence determine the fold point correction, as a function of β.

In the special case where the cooling pellet or rod is concentric with the outer boundary, the asymptotic results for the fold corrections in various cases can be compared with the numerical solution of the full problem (1.2a, b, c). To determine the location of the fold point as a function of ϵ from the full problem, in the case of concentric spheres or circles, we write (1.2a, b, c) as

$$u'' + \frac{(m-1)}{r} u' + \lambda F(u, \beta) = 0, \qquad F(u, \beta) = \exp(u/(1 + \beta u)), \tag{4.2a}$$

$$u' + b u = 0, \quad \text{on} \quad r = 1, \tag{4.2b}$$

$$-\epsilon u' + \kappa u = 0, \quad \text{on} \quad r = \epsilon, \tag{4.2c}$$

$$u' = -\gamma \quad \text{on} \quad r = 1, \qquad \gamma > 0. \tag{4.2d}$$

In (4.2c) we have assumed that D_ϵ has radius ϵ.

For fixed β and ϵ, the boundary value problem (4.2) is solved numerically for $u(r,\gamma)$ and $\lambda(\gamma)$ using COLSYS and a simple continuation scheme in γ. To determine the location of the first fold point accurately, we solve (4.2) subject to the side condition $\lambda'(\gamma_0) = 0$ and $\lambda'(\gamma) > 0$ for $\gamma < \gamma_0$. The value of λ at the first fold point is then labeled by $\lambda_c \equiv \lambda(\gamma_0)$. Finally, a simple continuation scheme in both ϵ and β is then used to determine the first fold point as a function of these two parameters.

We now compare our asymptotic predictions for the location of the first fold point, obtained using (4.1) and the results of §2.1 and §2.2, with the corresponding numerical values found from the full problem (4.2).

Spherical and Circular Cylindrical Reactors: Results

Using the numerical procedures outlined above, we now determine both asymptotically and numerically the correction to the fold point for a *spherical* reactor of radius one containing a concentric cooling or insulating pellet. In the calculations below, we take D_ϵ to be a sphere of radius ϵ located at the origin so that $r_0 = |x_0| = 0$.

For a perfect cooling pellet, where $\kappa = \infty$ and $C(\infty) = 1$, the asymptotic result for the fold point correction is given in (2.13a,b). Noting from (4.1d) that $u_0(0,\alpha) = \alpha$, then (2.13a,b) becomes

$$\lambda_c = \lambda_0(\alpha_0) + \epsilon\,\lambda_1(\alpha_0) + \cdots, \qquad \lambda_1(\alpha_0) = \frac{\alpha_0}{\int_0^1 r^2\, u_{0\alpha}(r,\alpha_0)\, F[u_0(r,\alpha_0),\beta]\, dr}. \tag{4.3a}$$

Here, the Arrhenius heating term, F, is specified in (4.1a).

Alternatively, if the spherical pellet of radius ϵ is insulating so that $\kappa = 0$, then the asymptotic result for the fold point correction is found from (2.16) and (2.17a,b). Assuming again that the pellet is located at the origin, from (2.16) and (2.17a,b) we obtain that

$$\lambda_c = \lambda_0(\alpha_0) + \epsilon^3\,\lambda_1(\alpha_0) + \cdots, \qquad \lambda_1(\alpha_0) = \frac{\lambda_0(\alpha_0)}{3}\frac{F(\alpha_0,\beta)}{\int_0^1 r^2\, u_{0\alpha}(r,\alpha_0)\, F[u_0(r,\alpha_0),\beta]\, dr}. \tag{4.3b}$$

Since $\lambda_1(\alpha_0) > 0$ in (4.3a) and (4.3b), the effect of such cooling and insulating pellets is to delay the onset of thermal runaway.

Numerical results for $\lambda_0(\alpha_0)$ and $\lambda_1(\alpha_0)$ for different β values in the case of cooling and insulating pellets, obtained from (4.1) and (4.3a,b), are shown in Table 1 for the case $b = \infty$. For this problem, the critical value of β for which multiple steady state solutions of (1.1) exist is roughly $\beta_c(\infty) \approx .2388$ (see Boddington et al. (1983)). In Table 3 we compare, at a fixed β value, the asymptotic and numerical values for $\lambda_c(\epsilon)$ obtained from (4.3a,b) and (4.2), respectively. The agreement between the asymptotic and numerical results is seen to be rather good even for only moderately small values of ϵ. In Fig. 3 we display our results of $\lambda_c(\epsilon)$ versus ϵ, for a cooling pellet, at different β values. The solid lines in the figure are the asymptotic results and the labeled points are the corresponding numerical values obtained from (4.2). The agreement between the asymptotic and numerical values for λ_c is seen from this figure to be uniform in β.

We now consider the two dimensional case of a *circular cylindrical* reactor of radius one containing a concentric cooling or insulating rod located at the origin. For the comparison of our asymptotic and numerical results for λ_c, in the calculations below we take D_ϵ to be a circular region of radius ϵ and we specify $b = \infty$ in (4.1) and (4.2).

For a cooling rod, the leading order asymptotic correction to the fold point is given by (2.22a,b) and is independent of κ. Noting from (4.1d) that $u_0(0,\alpha) = \alpha$, then (2.22a,b) becomes

$$\lambda_c = \lambda_0(\alpha_0) + (-\frac{1}{\log\epsilon})\,\lambda_1(\alpha_0) + \cdots, \qquad \lambda_1(\alpha_0) = \frac{\alpha_0}{\int_0^1 r\,u_{0\alpha}(r,\alpha_0)\,F[u_0(r,\alpha_0),\beta]\,dr}. \tag{4.4a}$$

Alternatively, for an insulating rod ($\kappa = 0$) the leading order asymptotic result for the correction to the fold point is found from (2.24) and (2.25a,b). For an insulating rod of area $\pi\epsilon^2$ centered at the origin, (2.25a,b) becomes

$$\lambda_c = \lambda_0(\alpha_0) + \epsilon^2\,\lambda_1(\alpha_0) + \cdots, \qquad \lambda_1(\alpha_0) = \frac{\lambda_0(\alpha_0)}{2}\frac{F(\alpha_0,\beta)}{\int_0^1 r\,u_{0\alpha}(r,\alpha_0)\,F[u_0(r,\alpha_0),\beta]\,dr}. \tag{4.4b}$$

Numerical results for $\lambda_0(\alpha_0)$ and $\lambda_1(\alpha_0)$ for different β values in the case of cooling and insulating rods, obtained from (4.1) and (4.4a,b), are shown in Table 2. The critical value of β in this case is roughly $\beta_c \approx .2421$, (see Boddington et al. (1983)). In Table 4 we compare, at a fixed β value, the asymptotic and numerical values for $\lambda_c(\epsilon)$ obtained from

$(4.3a,b)$ and (4.2), respectively. The agreement between the asymptotic and numerical results is seen to be rather good for insulating rods but is only fair for cooling rods. This rather poor agreement, with moderate values of ϵ, for cooling rods is a result of the expansion of λ_c in powers of $(-1/\log\epsilon)$ in this case. In Fig. 4 we display our results of $\lambda_c(\epsilon)$ versus ϵ, for an insulating rod, at different β values. The agreement between the asymptotic and numerical values for λ_c is again uniform in β.

For pellets and rods that are not concentric with D, a similar procedure using (4.1) and the asymptotic results of §2.1 and §2.2 can be used to determine the leading order fold correction. As an interesting application, consider the case of a small *insulating* spherical pellet or circular rod of radius ϵ placed inside a spherical or circular cylindrical reactor of radius one at some radius $r_0 \in [0,1)$. From $(2.17a,b)$ and $(2.25a,b)$, it follows that $\lambda_c = \lambda_0(\alpha_0) + \epsilon^{m-1}\,\lambda_1(\alpha_0) + \cdots$, where

$$\lambda_1(\alpha_0) = 2\pi(1-\frac{1}{m})\,\frac{u_{0\alpha}(r_0,\alpha_0)\lambda_0(\alpha_0)\,F[u_0(r_0,\alpha_0),\beta] - m\,\partial_r u_{0\alpha}(r_0,\alpha_0)\,\partial_r u_0(r_0,\alpha_0)}{\int_0^1 r^{m-1}\,u_{0\alpha}(r,\alpha_0)\,F[u_0(r,\alpha_0),\beta]\,dr}\,. \tag{4.5a}$$

Here, $m = 2,3$ is the number of dimensions. Viewing $(4.5a)$ as a function of r_0, then $\lambda_1(\alpha_0) = 0$ if r_0 is a root of

$$u_{0\alpha}(r_0,\alpha_0)\,\lambda_0(\alpha_0)\,F[u_0(r_0,\alpha_0),\beta] - m\,\partial_r u_{0\alpha}(r_0,\alpha_0)\,\partial_r u_0(r_0,\alpha_0) = 0\,. \tag{4.5b}$$

If $u_0 = 0$ on $r = 1$, there exists a unique solution r_0^* to $(4.5b)$, depending on β and m, such that $\lambda_1(\alpha_0) = 0$. By solving (4.1) and $(4.5b)$ numerically with $\beta = 0$, we find $r_0^* = .4472$ for $m = 2$ and $r_0^* = .4035$ for $m = 3$.

This result is interpreted as follows. If placed in a region where heat production is large, the small insulating body will delay marginally the onset of thermal runaway by an amount proportional to the size of the region removed. However, as the insulating body is moved closer to the outer boundary, its main effect is to prevent some heat from escaping out of the reactor surface, and the reactor becomes less stable.

Almost Total Insulation

We now consider the case in both two and three dimensions where the outer boundary of the reactor is perfectly insulated ($b = 0$). We first consider the three dimensional case

where we assume that a cooling pellet with $\kappa \neq 0$ is located at the center of a reactive sphere of radius one. We now show, in this special case, how to extend the leading order result (2.19) for $\lambda(\alpha)$ to one higher order.

To determine the next term in the expansion of λ, in the *outer* region away from ∂D_ϵ we write

$$u = \alpha + \epsilon u_1 + \epsilon^2 u_2 + \cdots, \qquad \lambda = \epsilon \lambda_1 + \epsilon^2 \lambda_2 + \cdots,$$

so that from (1.2a,b), u_1 and u_2 solve

$$\Delta u_1 = -\lambda_1 F(\alpha,\beta) \quad \text{in} \quad 0 < r < 1, \quad u_{1r} = 0 \quad \text{on} \quad r = 1. \tag{4.6a}$$

$$\Delta u_2 = -\lambda_2 F(\alpha,\beta) - \lambda_1 u_1 F_u(\alpha,\beta) \quad \text{in} \quad 0 < r < 1, \quad u_{2r} = 0 \quad \text{on} \quad r = 1. \tag{4.6b}$$

In the *inner* region we write $y = x/\epsilon$, $v(y) = u(\epsilon x)$ and expand $v = v_0 + \epsilon v_1 + \cdots$. Substituting this expansion in (2.4) we find that v_0 satisfies (2.6) and that v_1 satisfies the first equation of (2.14). The solution to (2.6) with $v_0 \to \alpha$ as $y \to \infty$ has the asymptotic form

$$v_0(y) \sim \alpha\Big[1 - \frac{C(\kappa)}{|y|} + \frac{P_i(\kappa)\, y_i}{|y|^3} + \cdots\Big] \quad \text{as} \quad |y| \to \infty. \tag{4.7}$$

Furthermore, since $\partial_{x_i}\alpha = 0$, we can choose $v_1 \equiv 0$.

Writing (4.7) in outer variables $x = \epsilon y$, then from the matching condition (2.7) we require that

$$u_1 \sim -\frac{\alpha\, C(\kappa)}{r}, \qquad u_2 \sim \alpha\, \frac{P_i(\kappa)\, x_i}{r^3} \qquad \text{as} \quad r = |x| \to 0. \tag{4.8}$$

A solution to (4.6a) subject to (4.8) exists only when λ_1 is given by (2.19). With λ_1 given in (2.19) we solve (4.6a) and (4.8) explicitly for u_1 to obtain

$$u_1 = -\frac{C(\kappa)\,\alpha}{r} - \frac{C(\kappa)\,\alpha\, r^2}{2}. \tag{4.9}$$

In deriving (4.9) we have made u_1 unique by specifying $u_1 + \alpha C(\kappa)/r \to 0$ as $r \to 0$.

With λ_1 and u_1 known, we now determine λ_2 from (4.6b) and (4.8). To incorporate the required singular behavior for u_2 we write (4.6b) as

$$\begin{aligned} &\Delta u_2 = -\lambda_2 F(\alpha,\beta) - \lambda_1 u_1 F_u(\alpha,\beta) - 4\pi\,\alpha\, P_i\, \partial_{x_i}\delta(x) \quad \text{in} \ 0 < r < 1, \\ &u_{2r} = 0 \quad \text{on} \ r = 1, \end{aligned} \tag{4.10}$$

where $\delta(x)$ is the Dirac delta function. Invoking a solvability condition on (4.10) and using (2.19) and (4.9) for λ_1 and u_1, respectively, we readily derive an equation for $\lambda_2(\alpha)$. To two terms, with $F(u,\beta) = \exp(u/(1+\beta u))$, we have $\lambda(\alpha) = \epsilon\lambda_1(\alpha) + \epsilon^2\lambda_2(\alpha) + \cdots$, where

$$\lambda_1(\alpha) = 3\,C(\kappa)\,\alpha\,\exp(-\alpha/(1+\beta\alpha))\,, \qquad \lambda_2(\alpha) = \frac{27}{5}\frac{(C(\kappa)\,\alpha)^2}{(1+\alpha\beta)^2}\,\exp(-\alpha/(1+\beta\alpha))\,. \tag{4.11}$$

Setting $\lambda_1'(\alpha_0) = 0$ and choosing the smallest such root to obtain the first fold point, we find that

$$\alpha_0 = \frac{1}{2\beta^2}[(1-2\beta) - (1-4\beta)^{1/2}]\,. \tag{4.12}$$

It follows that for $\beta > .25$ the graph of α versus λ is monotone for $\epsilon \ll 1$. For $\beta < .25$, however, we have that $\lambda_c \equiv \lambda(\alpha_0)$ with $\lambda(\alpha)$ given above specifies the location of the first fold point. As a special case, when $\beta \to 0$ then $\alpha_0 \to 1$ and so from (4.11) we obtain that

$$\lambda_c = 3\,\epsilon\,C(\kappa)\,e^{-1} + \frac{27\epsilon^2}{5}\,(C(\kappa))^2\,e^{-1} + \cdots\,, \qquad \beta = 0\,. \tag{4.13}$$

We now choose D_ϵ to be a sphere of radius ϵ centered at the origin and in (2.6) we specify $\kappa = 1$ so that $C(1) = .50$. In this special case, the one and two term asymptotic results from (4.13) are compared with numerical values for $\lambda_c(\epsilon)$ obtained from the full problem (4.2). As seen in Table 5, where these results are shown, the agreement between the two term asymptotic result and the numerical result is good even for moderately small values of ϵ.

Similar results can be obtained in the two-dimensional case when the outer boundary is perfectly insulating. We now take D to be a circular cylindrical reactor of radius one containing a concentric cooling rod of arbitrary cross section. In this case, it is again possible to extend the leading order result (2.27) to one higher order by a procedure similar to that used above in the three dimensional case. Omitting the details of the calculation, we find that

$$\lambda(\alpha) = (-\frac{1}{\log\epsilon})\,2\alpha\,\exp(-\alpha/(1+\beta\alpha))\Big(1-(-\frac{1}{\log\epsilon})\,\frac{\alpha}{(1+\alpha\beta)^2}\,(d(\kappa)-3/4)+\cdots\Big)\,. \tag{4.14}$$

Here, $d(\kappa)$ is found from (2.20).

If $\beta < .25$ then the first fold point is located at $\lambda_c \equiv \lambda(\alpha_0)$ where α_0 is given in (4.12). If $\beta \to 0$ then $\alpha_0 \to 1$ and so from (4.14) we have that

$$\lambda_c = (-\frac{1}{\log \epsilon}) 2e^{-1} - (-\frac{1}{\log \epsilon})^2 2(d(\kappa) - 3/4)\, e^{-1} + \cdots . \tag{4.15}$$

Taking D_ϵ to be a circle of radius ϵ with $\kappa = 1$, so that $d(1) = 1$, in Table 6 the one and two term asymptotic results from (4.15) are compared with numerical values for $\lambda_c(\epsilon)$ obtained from (4.2), with clear agreement.

5 Boundary Perturbations: Comparison of Asymptotics and Numerics

We now apply the results of §3 to determine the effect of small cooling and insulating segments (2-D) and patches (3-D) on a model chemical reactor with a nonlinear heat generation term given by (4.1a).

A Slab Reactor: $\beta = 0$

For our first problem we consider a slab reactor in the rectangle $-L < x < L$, $0 < y < 1$, with a small insulating segment on one side. The temperature, u, for the perturbed problem is taken to satisfy

$$\begin{aligned} &\Delta u + \lambda F(u,\beta) = 0\,, \qquad -L < x < L\,,\ 0 < y < 1 \\ u_x = 0 \quad &\text{on } x = -L,\, L; \qquad u_y = 0 \quad \text{on } y = 0 \\ u = 0 \quad &\text{on } y = 1\,,\ |x| > \epsilon; \qquad u_y = 0 \quad \text{on } y = 1\,,\ |x| < \epsilon\,. \end{aligned} \tag{5.1}$$

For $\beta = 0$ and $L = \infty$, (5.1) was previously considered by Adler (1983) and Herbert (1986), who produce contradictory analytical expressions for $\lambda_c(\epsilon)$ when $\epsilon \ll 1$. For these parameter values, Adler derived $\lambda_c = .87846(1 - \epsilon + \cdots)$ while Herbert derived $\lambda_c = .87846(1 - .0549\,\epsilon^2 + \cdots)$, both results predicting a nonvanishing correction to the unperturbed fold point when $L = \infty$. The slab reactor (5.1) was also treated numerically by Greenway and Spence (1985) for $L = 10$ and for various values of ϵ. They concluded that their results for $\lambda_c(\epsilon)$ and $L = 10$ also apply to the case $L = \infty$, and so they also predicted a nonvanishing correction to the fold point for an infinite slab. Their numerical results for $\lambda_c(\epsilon)$ disagreed substantially from Adler's prediction and were inconclusive with regards to Herbert's result.

More recently Ward and Keller (1990), using the analytical theory presented in §3, have conjectured that $\lambda_c = .87846(1 - 1.571\epsilon^2/L + \cdots)$ for the case $\beta = 0$. This result disagrees qualitatively with that of Herbert and Adler in that the correction to the fold point of order $O(\epsilon^2)$ vanishes as $L \to \infty$. When $L = 10$ this result was also only in fair agreement with the numerical results of Greenway and Spence, but did agree more closely than Herbert's result.

We now give some numerical evidence to support the conjecture of Ward and Keller by solving (5.1) numerically for various values of ϵ and L on a finer mesh than that used in Greenway and Spence. In addition, we also extend the analytical results of Ward and Keller to treat the case $\beta > 0$. The asymptotic predictions for $\lambda_c(\epsilon)$ when $\beta \geq 0$ are then compared to numerical results obtained from (5.1) for the finite slab, and clear agreement is found. We first outline our numerical method to treat (5.1).

Numerical Solution of the Slab Reactor

For our numerical computations, we chose methods that were readily available to us; efficient hardware use was not a primary objective. Computation times were kept reasonable through concurrent computing: all computations were done on Caltech's Symult Series 2010 multicomputer, which has 192 processors. Path following was done with the concurrent continuation method of Van de Velde and Lorenz (1989), which implements Keller's (1987) arclength-continuation method and is based on direct solvers. More efficient procedures are possible if one exploits the elliptic nature of the underlying problem and/or if one uses specialized procedures to follow folds (see Fier (1985), e.g.). We assessed the accuracy of our discretizations and their computed solutions by varying the grid size and the order of discretization.

We impose the symmetry of problem (5.1) with respect to the y-axis. This reduces our computational domain to the rectangle $[0, L] \times [0, 1]$. Along the edge $x = 0$ a homogeneous Neumann boundary condition is imposed to enforce the symmetry. A regular grid consisting of $h \times h$ square grid cells covers the domain. We used two different discretizations of the interior operator: the standard second order five point difference scheme and Collatz's fourth order Mehrstellenverfahren (see Collatz (1966)). The Dirichlet boundary

conditions are naturally imposed at the boundary points. The Neumann boundary conditions are discretized to second order accuracy by the standard procedure of introducing an artificial boundary, imposing the interior operator on the real boundary, and subsequently eliminating the artificial boundary with the Neumann boundary condition.

The resulting discrete problem has the form $G(\mathbf{u}, \mu) = 0$, where G is a mapping from $R^M \times R \to R$, $\mathbf{u} \in R^M$, $\mu \in R$, and the dimension M is the number of unknowns in the problem. In our case, the parameter μ could be λ, β, or ϵ, although we only performed continuations in λ. The concurrent continuation program is used to compute solution paths $(\mathbf{u}(s), \mu(s))$, where s is a pseudo-arclength. When continuing in λ, we stop the continuation after detection of the first fold.

To do meaningful continuations in ϵ, the number of unknowns must be independent of ϵ. To achieve this, Greenway and Spence (1985) use a staggered grid without any grid points on the domain boundary. As a result, however, an $O(h)$ discretization error is introduced on the Dirichlet boundary conditions. We chose, instead, not to eliminate those (trivial) equations that correspond to Dirichlet boundary points. In this way, the same goal (a number of unknowns independent of ϵ) is achieved, without incurring a larger discretization error. We point out that Greenway and Spence alleviate the problem somewhat by using a locally graded mesh. Hence, their local discretization step $h_{i,j}$ in the neighborhood of the Dirichlet boundary is less than our discretization step h (here, we compare grids with the same number of points).

There is one $O(h)$ discretization error remaining in our and Greenway and Spence's scheme, however, because the length ϵ is approximated by a multiple of the grid size h. When ϵ is not an exact multiple of h, an $O(h)$ error in approximating ϵ is made. To minimize this error, we restrict values of ϵ to multiples of h.

To asses the accuracy of the discretization, we performed several tests. First, we tested for convergence under grid refinement. In Fig. 5, projections of solution paths $(\mathbf{u}, \lambda)$ of fourth order discretizations of (5.1) are plotted. (Note: $L = 2.0$, $\epsilon = 0.1$, and $\beta = 0$. The maximum norm of $\mathbf{u}$ is plotted along the y-axis.) Solution paths were computed for the discrete systems approximating (5.1) with discretization steps $h = 1/10, 1/20, 1/30$, and $1/40$, respectively. The paths of the discrete systems were computed to an accuracy of

10^{-6}. The plot in Fig. 5 is a blow-up of the neighborhood of the fold, which is the part of the solution path that is most sensitive with respect to changes in h. Away from the fold, all solution paths, except for the one corresponding to $h = 1/10$, collapse into one curve (not shown). Since the computed λ_c increases with decreasing h, it is a reasonable assumption that, through discretization, the location of the fold of the continuous system is underestimated. As a trade-off between accuracy and computing time, we chose $h = 1/20$ for most of our computations. With this grid, we expect that λ_c is computed with an accuracy of at least two significant digits.

As a further test, we compared computations with a different order of approximation of the interior operator. Fig. 6 shows only marginal influence on the computed solution path for all values of λ. This indicates that errors other than the discretization error of the interior operator are dominant. We note that it is difficult to compare the results on a more quantitative basis, e.g., by considering the relative difference between solutions, because different points along the path are computed with each discretization.

A contour plot of the solution in the neighborhood of the fold with $L = 10$, $\epsilon = 0.1$ and $\beta = 0$, is shown in Fig. 7. This figure gives a visual and qualitative indication that sufficient resolution is obtained with $h = 1/20$. We note that this figure is scaled differently in the x and y directions. The square plot is actually a representation of a 10×1 rectangle.

In Fig. 8 we plot the solution paths in the neighborhood of the fold point when $\beta = 0$, $\epsilon = 0.1$ and $L = 1, 2, 3, 5, 10$. The solid line connects the computed fold points. In Table 7a we compare the location of the fold points as predicted by the asymptotic analysis with those computed numerically for different L values, obtaining clear agreement. In Table 7b we compare the asymptotic and numerical results for $\lambda_c(\epsilon)$ for different ϵ values with $\beta = 0$ and $L = 5$. To keep ϵ an exact multiple of h, the computations for $\epsilon = 0.1$ were done with $h = 1/20$, while for $\epsilon = 0.08$ and $\epsilon = 0.12$ we used $h = 1/25$. Although the changes in λ_c occur in the third digit, which may be beyond the accuracy of the numerical computations, it is clear that the discrete system behaves qualitatively like the asymptotically approximated continuous system.

Our numerical evidence obtained by solving (5.1) numerically for different L and ϵ values, strongly supports the conjecture that $\lambda_c(\epsilon) = .87846(1 - 1.571\epsilon^2/L + \cdots)$ for the

case $\beta = 0$ and finite L. However, since it is not possible to compute the solution to (5.1) for arbitrarily large L values or arbitrarily small ϵ values, we cannot conclusively rule out the predictions of Adler or Herbert. The support for our conjecture rests mainly on the comparisons of the asymptotic and numerical values of $\lambda_c(\epsilon)$ for the finite slab. Additional support is derived from our extensive testing of the general theory for the determination of λ_c performed in §4 in the case of an interior perturbation.

A Slab Reactor: $\beta > 0$

We now extend our analytical results by determining the correction to the first fold point of (5.1) for the case $\beta > 0$. Since the unperturbed solution, $u_0(y)$, for (5.1) is independent of x, the extended system obtained from (1.1) and (2.9) is chosen as

$$\begin{aligned} u_0'' + \lambda_0 F(u_0,\beta) &= 0, \qquad 0 < y < 1 \\ u_{0\alpha}'' + \lambda_0 F_u(u_0,\beta)\, u_{0\alpha} &= -\lambda_0' F(u_0,\beta), \qquad 0 < y < 1 \\ u_0'(0) = 0, \qquad u_0(1) &= 0, \qquad u_0(0) = \alpha, \\ u_{0\alpha}'(0) = 0, \qquad u_{0\alpha}(1) &= 0, \qquad u_{0\alpha}(0) = 1. \end{aligned} \tag{5.2}$$

Only when $\beta = 0$ can a closed form analytical solution to (5.2) be found. Otherwise the unperturbed problem (5.2) must be solved numerically to locate the first fold point, by a method similar to that described in §4. Then the expansion of the fold point for $\epsilon \ll 1$, given in (3.7), can be written as

$$\lambda_c = \lambda_0(\alpha_0) + \frac{\epsilon^2\, \hat{\lambda}_1(\alpha_0)}{L} + \cdots, \qquad \hat{\lambda}_1(\alpha_0) = -\frac{\pi}{4} \frac{u_{0\alpha}'(1,\alpha_0)\, u_0'(1,\alpha_0)}{\int_0^1 u_{0\alpha}(y,\alpha_0)\, F[u_0(y,\alpha_0),\beta]\, dy}. \tag{5.3}$$

Numerical values for $\lambda_0(\alpha_0)$ and $\hat{\lambda}_1(\alpha_0)$ at different β values are given in Table 8. In Fig. 9 and Table 9 we compare the values of λ_c as predicted by the asymptotic analysis with those computed numerically, for $L = 5.0$, $\epsilon = 0.1$, and a range of values for β. The numerical computations were performed with $h = 1/20$. The numerically computed values of λ_c slightly underestimate the values obtained by the asymptotic analysis. This is in line with our earlier observation that solution paths of coarser discretizations become critical sooner than those of finer grids. The rather good agreement between the asymptotic

and numerical results for $\lambda_c(\epsilon)$ further supports our conjecture that for $0 \le \beta \le \beta_c$ we have $\lambda_c(\epsilon) - \lambda_0(\alpha_0) = o(\epsilon^2)$ for an infinite slab with $L = \infty$. An unsolved problem is to determine whether $\lambda_c(\epsilon) - \lambda_0(\alpha_0) = o(\epsilon^p)$ for any power $p > 0$ for the infinite slab.

The results of §3 can be used to treat other reactors. In particular, let D be a rectangular box reactor with a circular insulating patch on one face so that

$$\Delta u + \lambda F(u,\beta) = 0 \quad \text{in } 0 \le x \le L_x\,,\ \ 0 \le y \le 1\,,\ \ 0 \le z \le L_z\,,$$
$$\partial_z u = 0 \text{ on } z = 0,\, L_z\,; \quad \partial_x u = 0 \text{ on } x = 0,\, L_x\,; \quad \partial_y u = 0 \text{ on } y = 0\,,$$
$$u = 0 \quad \text{on } y = 1,\ (x,z) \notin \partial D_\epsilon\,; \quad \partial_y u = 0 \quad \text{on } y = 1,\ (x,z) \in \partial D_\epsilon\,.$$

Here, ∂D_ϵ is a circular patch of radius ϵ centered at $(x_0, 1, z_0)$ and $F(u,\beta)$ is given in (4.1a). When $\beta = 0$ this problem was considered by Zaturska (1984), who used Adler's method to produce an $O(\epsilon)$ correction to the location of the fold point. Our result below, however, predicts an $O(\epsilon^3)$ correction to the fold point.

Since the solution, $u_0(y)$, to the unperturbed problem is the same as for the two-dimensional slab considered in (5.1), we find from (3.16) and (3.17) that

$$\lambda_c = \lambda_0(\alpha_0) + \frac{16}{3\pi}\,\frac{\hat{\lambda}_1(\alpha_0)}{L_x\,L_z}\,\epsilon^3 + \cdots\,.$$

Here $\lambda_0(\alpha_0)$ and $\hat{\lambda}_1(\alpha_0)$, defined in (5.3), are tabulated for different β values in Table 8.

A Spherical Reactor

We now determine numerical values for the asymptotic results of §3.2 for a spherical reactor of radius one that has either an insulating or cooling patch on its boundary. In (1.3) we assume that the projection of the cooling or insulating patch onto the tangent plane at x_0 is a circle of radius ϵ.

For the case of a circular insulating patch, with $b = \infty$ and $\kappa = 0$, we find from (3.16) and (3.17) that

$$\lambda_c = \lambda_0(\alpha_0) + \epsilon^3\lambda_1(\alpha_0) + \cdots\,, \qquad \lambda_1(\alpha_0) = -\frac{1}{3\pi}\,\frac{u_{0\alpha}'(1,\alpha_0)\,u_0'(1,\alpha_0)}{\int_D r^2\,u_{0\alpha}(r,\alpha_0)\,F[u_0(r,\alpha_0),\beta]\,dr}\,. \tag{5.4a}$$

For the case of a circular cooling patch, with $b = 1$ and $\kappa = \infty$, we find from (3.14) and (3.15) that

$$\lambda_c = \lambda_0(\alpha_0) + \epsilon\lambda_1(\alpha_0) + \cdots, \qquad \lambda_1(\alpha_0) = \frac{1}{\pi} \frac{u_{0\alpha}(1,\alpha_0)\, u_0(1,\alpha_0)}{\int_D r^2\, u_{0\alpha}(r,\alpha_0)\, F[u_0(r,\alpha_0),\beta]\, dr}. \quad (5.4b)$$

As an illustration, the unknown quantities appearing in (5.4a) and (5.4b) are found from the numerical solution to the extended system (4.1) with $b = \infty$ and $b = 1$, respectively, and with $m = 3$. The resulting numerical values for $\lambda_0(\alpha_0)$ and $\lambda_1(\alpha_0)$ are given in Table 10.

We have not solved the fully three-dimensional perturbed problem (1.3) numerically in the case of insulating or cooling patches on the boundary. However, we anticipate that the agreement between the numerical and asymptotic results would be similar to the case of a concentric insulating or cooling pellet, which was examined in §4.

A Circular Cylindrical Reactor

We now determine numerical values for the asymptotic results of §3.1 for a circular cylindrical reactor of radius one that has either an insulating or cooling segment, of length 2ϵ on its boundary.

For the case of an insulating segment, with $b = \infty$ and $\kappa = 0$, we find from (3.7) that

$$\lambda_c = \lambda_0(\alpha_0) + \epsilon\lambda_1(\alpha_0) + \cdots, \qquad \lambda_1(\alpha_0) = -\frac{1}{4} \frac{u'_{0\alpha}(1,\alpha_0)\, u'_0(1,\alpha_0)}{\int_D r\, u_{0\alpha}(r,\alpha_0)\, F[u_0(r,\alpha_0),\beta]\, dr}. \quad (5.5a)$$

Alternatively for the case of a cooling segment, with $b = 1$ and $\kappa = \infty$, we find from (3.5) that

$$\lambda_c = \lambda_0(\alpha_0) + (-\frac{1}{\log\epsilon})\lambda_1(\alpha_0) + \cdots, \qquad \lambda_1(\alpha_0) = \frac{1}{2} \frac{u_{0\alpha}(1,\alpha_0)\, u_0(1,\alpha_0)}{\int_D r\, u_{0\alpha}(r,\alpha_0)\, F[u_0(r,\alpha_0),\beta]\, dr}. \quad (5.5b)$$

As an example, the unknown quantities appearing in (5.5a) and (5.5b) are found from the numerical solution to the extended system (4.1) with $b = \infty$ and $b = 1$, respectively, and with $m = 2$. Numerical values for $\lambda_0(\alpha_0)$ and $\lambda_1(\alpha_0)$ are given in Table 11.

Although we have not compared (5.5a, b) with the numerical solution to (1.3), we anticipate a similar agreement between the numerical and asymptotic results for $\lambda_c(\epsilon)$ as was obtained in §4 for concentric cooling or insulating rods.

Discussion

We close with two remarks. Since the theory to treat boundary perturbations is only a slight modification of that used to examine interior domain perturbations, the rather extensive validation of the asymptotic theory in §4 for various ranges of b and κ provides a partial check on the results in §5. Therefore, although we compared our asymptotic and numerical results in §5 only for a finite slab reactor, for reactors of other geometries and other ranges of b and κ, we anticipate a similar agreement as was obtained in §4.

For each of the examples presented in §4 and §5 the unperturbed solution can be found from a boundary value problem for ordinary differential equations. This restriction is not necessary in that for fully two or three dimensional problems a numerical solution to (1.1) can be used together with the asymptotic results of §2 and §3 to give the correction to the location of the fold point. In this way, we can treat reactors with arbitrary geometries and boundary conditions, while avoiding to solve numerically any highly stiff problems. The accuracy of the resulting expressions for $\lambda_c(\epsilon)$ for $\epsilon \ll 1$ would probably be similar to that found for the special cases considered in §4 and §5.

Acknowledgment

We would like to thank Prof. J. B. Keller for some helpful discussions.

References

J. Adler 1983, The Thermal Stability of a Partially Insulated Reactive Slab, Combustion and Flame 50, pp. 1-7.

U. Ascher, R. Christiansen, R. Russell 1979, Collocation Software for Boundary value ODE's, Math. Comp. 33, pp. 659-679.

J. Bebernes, D. Eberly 1990, Mathematical Problems from Combustion Theory, Appl. Math. Sciences 83, Springer Verlag, New York .

T. Boddington, C. Feng, P. Gray 1983, Thermal Explosions, Criticality and the Disappearance

of Criticality in Systems with Distributed Temperatures. 1. Arbitrary Biot Number and General Reaction-Rate Laws. Proc. Roy. Society of London, A 390 pp. 247-264.

L. Collatz 1966, The Numerical Treatment of Differential Equations, Springer Verlag, Berlin.

J. Fier 1985, Part 1: Fold Continuation and the Flow between Rotating Coaxial Disks, Ph.D. Thesis, Caltech.

P. Greenway, A. Spence 1985, Numerical Calculation of Critical Points for a Slab with Partial Insulation, Combustion and Flame 62, pp. 141-156.

D. M. Herbert 1986, The Thermal Stability of a Partially Insulated Reactive Slab, Q. J. of Mech. and Appl. Math. Vol. 39 Pt. 2 pp. 197-207.

H. B. Keller 1987, Numerical Methods in Bifurcation Problems, Tata Institute of Fundamental Research, Bombay.

E. F. Van de Velde, J. L. Lorenz 1989, Adaptive Data Distributions for Concurrent Continuation, Report CRPC-89-4, Caltech.

M. J. Ward, J. B. Keller 1990, Nonlinear Eigenvalue Problems under Strong Localized Perturbations with Applications to Chemical Reactors, Accepted, Studies in Appl. Math.

M. Zaturska 1984, Thermal Explosion Theory for Partially Insulated Reactants, Combustion and Flame 56, pp. 97-103.

β	$\lambda_0(\alpha_0)$	$\lambda_1(\alpha_0)$ (4.3a)	$\lambda_1(\alpha_0)$ (4.3b)
0.0000	3.322	8.079	27.77
0.0556	3.552	8.449	28.93
0.1111	3.837	8.891	30.29
0.1389	4.010	9.148	31.07
0.1667	4.212	9.437	31.92
0.1944	4.456	9.762	32.86
0.2222	4.773	10.12	33.82

Table 1: Spherical reactor containing a concentric cooling or insulating pellet: Asymptotic results

β	$\lambda_0(\alpha_0)$	$\lambda_1(\alpha_0)$ (4.4a)	$\lambda_1(\alpha_0)$ (4.4b)
0.0000	2.000	2.773	8.000
0.0444	2.104	2.899	8.368
0.0889	2.227	3.045	8.796
0.1111	2.297	2.877	9.038
0.1333	2.375	2.962	9.305
0.1556	2.463	3.056	9.602
0.1778	2.563	3.163	9.937

Table 2: Circular cylindrical reactor with a concentric cooling or insulating rod: Asymptotic results

ϵ	λ_c (4.2)	λ_c (4.3a)	ϵ	λ_c (4.2)	λ_c (4.3b)
0.050	4.303	4.282	0.050	3.841	3.838
0.075	4.558	4.504	0.100	3.865	3.846
0.100	4.831	4.726	0.125	3.891	3.854
0.125	5.127	4.948	0.150	3.927	3.867
0.150	5.447	5.171	0.200	4.037	3.908

Table 3: Spherical reactor containing a concentric cooling or insulating pellet: Comparison of asymptotic and numerical results, $\beta = .1111$

ϵ	λ_c (4.2)	λ_c (4.4a)	ϵ	λ_c (4.2)	λ_c (4.4b)
0.010	3.066	2.888	.050	2.249	2.249
0.025	3.336	3.053	.075	2.275	2.276
0.050	3.684	3.244	.100	2.312	2.315
0.075	4.002	3.403	.125	2.359	2.364
0.100	4.317	3.550	.150	2.417	2.429

Table 4: Circular cylindrical reactor with a concentric cooling or insulating rod: Comparison of asymptotic and numerical results, $\beta = .08889$

ϵ	$\lambda_c(\epsilon)$ (4.2)	λ_c (4.11) (1 term)	λ_c (4.11) (2 terms)
.010	.00557	.00552	.00557
.050	.02888	.02759	.02888
.100	.06052	.05518	.06015
.150	.09528	.08277	.09395
.200	.13359	.11036	.13023

Table 5: Spherical reactor with almost total insulation, $b = 0$, $\beta = 0$, $\kappa = 1$

ϵ	$\lambda_c(\epsilon)$ (4.2)	λ_c (4.13) (1 term)	λ_c (4.13) (2 terms)
.010	.1503	.1598	.1511
.050	.2227	.2456	.2251
.100	.2805	.3195	.2848
.150	.3308	.3878	.3367
.200	.3790	.4572	.3861

Table 6: Circular cylindrical reactor with almost total insulation, $b = 0$, $\beta = 0$, $\kappa = 1$

L	λ_c (asymptotics)	λ_c (numerics)	relative error
1.0	.8647	.8548	1.16 %
2.0	.8716	.8662	0.62 %
3.0	.8739	.8695	0.51 %
5.0	.8757	.8717	0.46 %
10.0	.8771	.8725	0.53 %

Table 7a: Slab Reactor with an insulating segment: Asymtptotic and numerical results for λ_c at different L values with $\beta = 0$, $\epsilon = 0.1$.

ϵ	λ_c (asymptotics)	λ_c (numerics)	relative error
0.08	.8767	.8748	0.22 %
0.10	.8757	.8717	0.46 %
0.12	.8739	.8703	0.42 %

Table 7b: Slab Reactor with an insulating segment: Asymptotic and numerical results for λ_c at different ϵ values with $\beta = 0$, $L = 5$.

β	$\lambda_0(\alpha_0)$	$\hat{\lambda_1}(\alpha_0)$ (5.3)
0.0000	.87846	-1.3799
0.0244	.90184	-1.4166
0.0489	.92720	-1.4564
0.0733	.95486	-1.4999
0.0978	.98529	-1.5477
0.1222	1.0191	-1.6008
0.1467	1.0571	-1.6605

Table 8: Slab Reactor with an insulating segment: Asymptotic results with $\beta \geq 0$

β	λ_c (5.3)	λ_c (5.1)
0.00000	.87570	.87173
0.02444	.89901	.89539
0.04889	.92428	.92061
0.07333	.95186	.94815
0.09778	.98219	.97844
0.12222	1.01590	1.01209
0.14667	1.05378	1.04994
0.17111	1.09714	1.09347
0.19556	1.14798	1.14431

Table 9: Slab Reactor with an insulating segment: Asymptotic and numerical results with $\epsilon = .10$, $L = 5$

β	$\lambda_0(\alpha_0)$ $(b = \infty)$	$\lambda_1(\alpha_0)$ (5.4a)	$\lambda_0(\alpha_0)$ $(b = 1)$	$\lambda_1(\alpha_0)$ (5.4b)
0.0000	3.322	-1.661	.901	.360
0.0556	3.552	-1.776	.957	.383
0.1111	3.837	-1.919	1.024	.412
0.1389	4.010	-2.005	1.065	.428
0.1667	4.212	-2.106	1.111	.448
0.1944	4.456	-2.228	1.167	.471
0.2222	4.773	-2.387	1.236	.500

Table 10: Spherical reactor with a circular cooling or insulating patch: Asymptotic results

β	$\lambda_0(\alpha_0)$ $(b=\infty)$	$\lambda_1(\alpha_0)$ $(5.5a)$	$\lambda_0(\alpha_0)$ $(b=1)$	$\lambda_1(\alpha_0)$ $(5.5b)$
0.0000	2.000	-1.000	.576	.220
0.0444	2.104	-1.052	.604	.231
0.0889	2.227	-1.114	.636	.244
0.1111	2.297	-1.149	.655	.252
0.1333	2.375	-1.188	.675	.260
0.1556	2.463	-1.232	.698	.269
0.1778	2.563	-1.282	.724	.279

Table 11: Circular cylindrical reactor with an insulating or cooling segment:

Asymptotic results

Figure Captions

Fig. 1 a: A schematic plot illustrating an interior domain perturbation.

Fig. 1 b: A schematic plot illustrating a strong localized boundary perturbation.

Fig. 2: A schematic plot of solution multiplicity for cylindrical reactors.

Fig. 3: Comparison of asymptotic and numerical values of $\lambda_c(\epsilon)$ for a spherical reactor.

Fig. 4: Comparison of asymptotic and numerical values of $\lambda_c(\epsilon)$ for a cylindrical reactor.

Fig. 5: Solution paths for fourth order discretizations of (5.1) with $L = 2.0$, $\epsilon = 0.1$, $\beta = 0$ computed with $h = 1/10, 1/20, 1/30, 1/40$.

Fig. 6: Solution paths for (5.1) with $L = 5.0$, $\epsilon = 0.1$, $\beta = 0.02444$ computed with $h = 1/20$ using second and fourth order discretizations.

Fig. 7: Contour plot of the solution to (5.1) with $L = 10$, $\epsilon = 0.1$, $\beta = 0$, and $\lambda \approx \lambda_c$, computed with $h = 1/20$ and a fourth order discretization.

Fig. 8: Solution paths in the neighborhood of the fold point for different L values with $\beta = 0$, $\epsilon = 0.1$, $h = 1/20$.

Fig. 9: Asymptotic and numerical predictions for λ_c for different β values with $L = 5.0$, $\epsilon = 0.1$, $h = 1/20$.

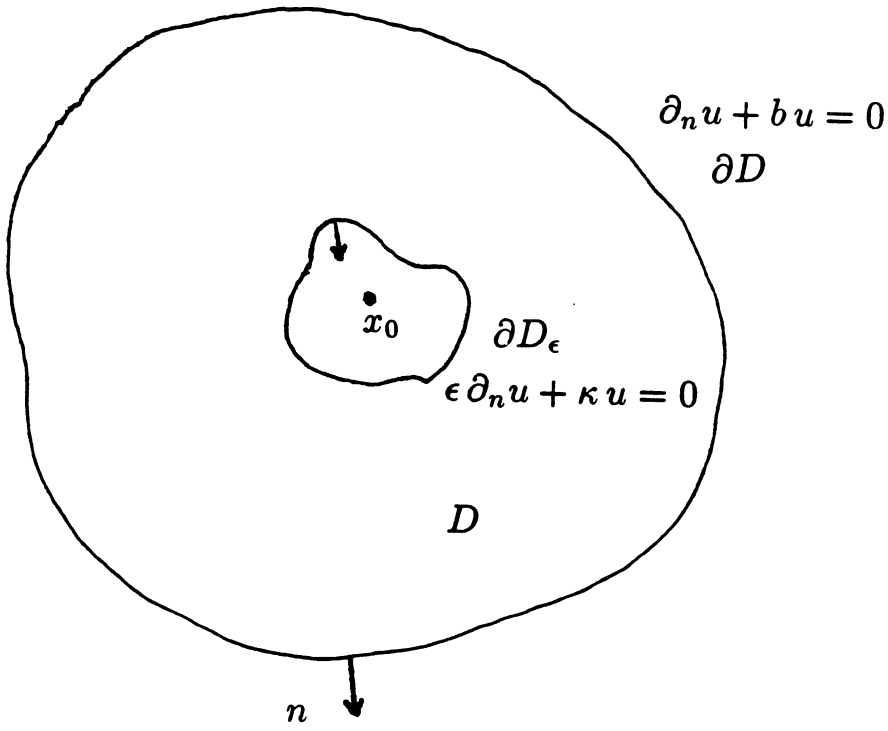

Figure 1a

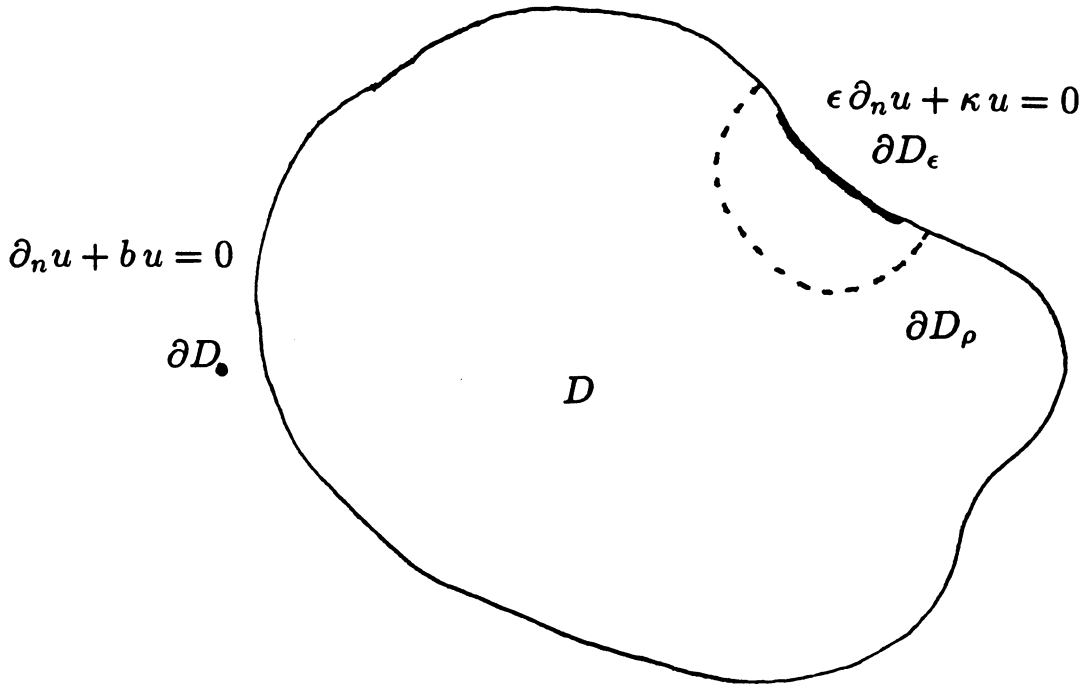

Figure 1b

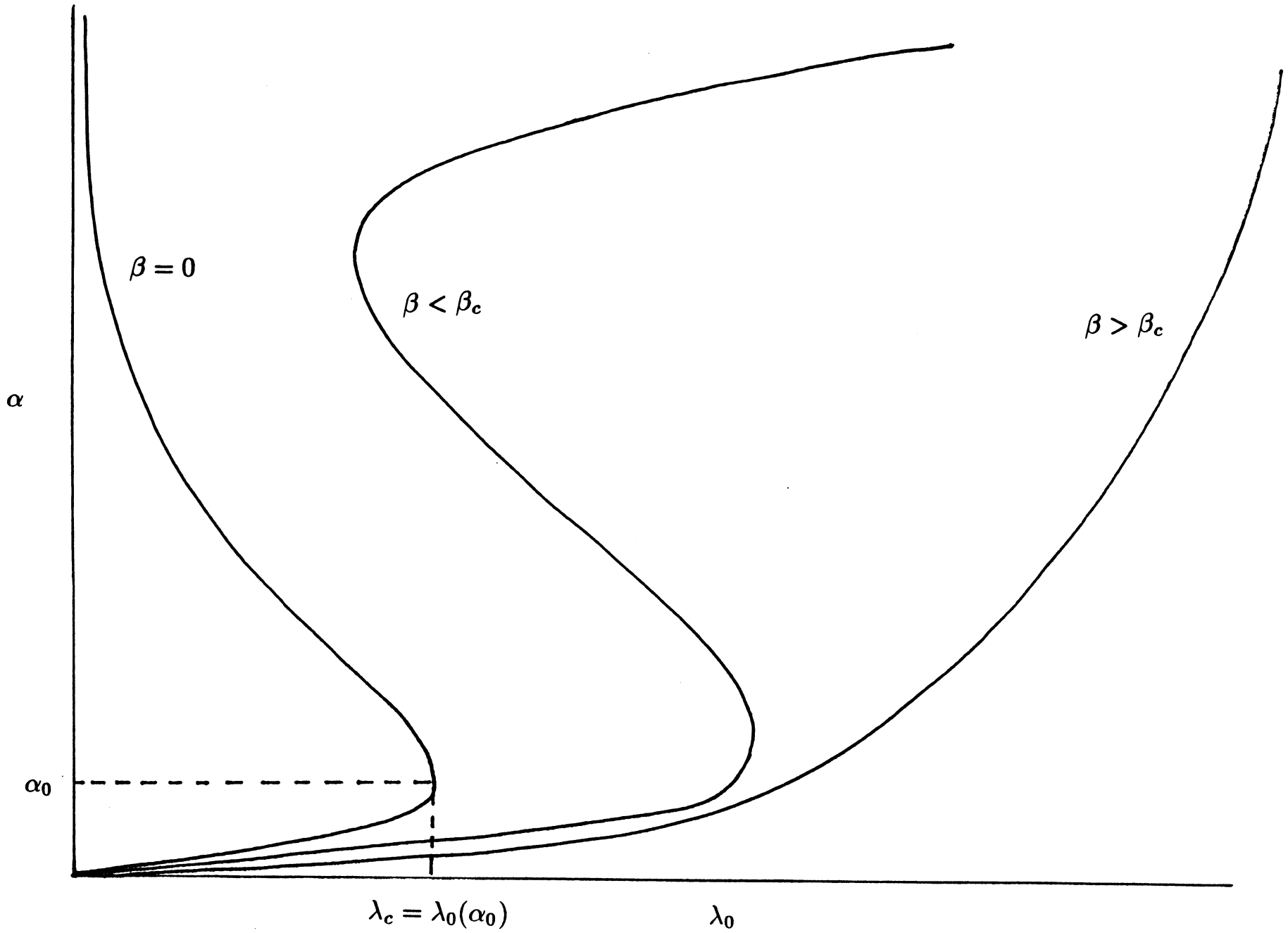
$\beta = 0$
$\beta < \beta_c$
$\beta > \beta_c$
α
α_0
$\lambda_c = \lambda_0(\alpha_0)$
λ_0

Figure 2

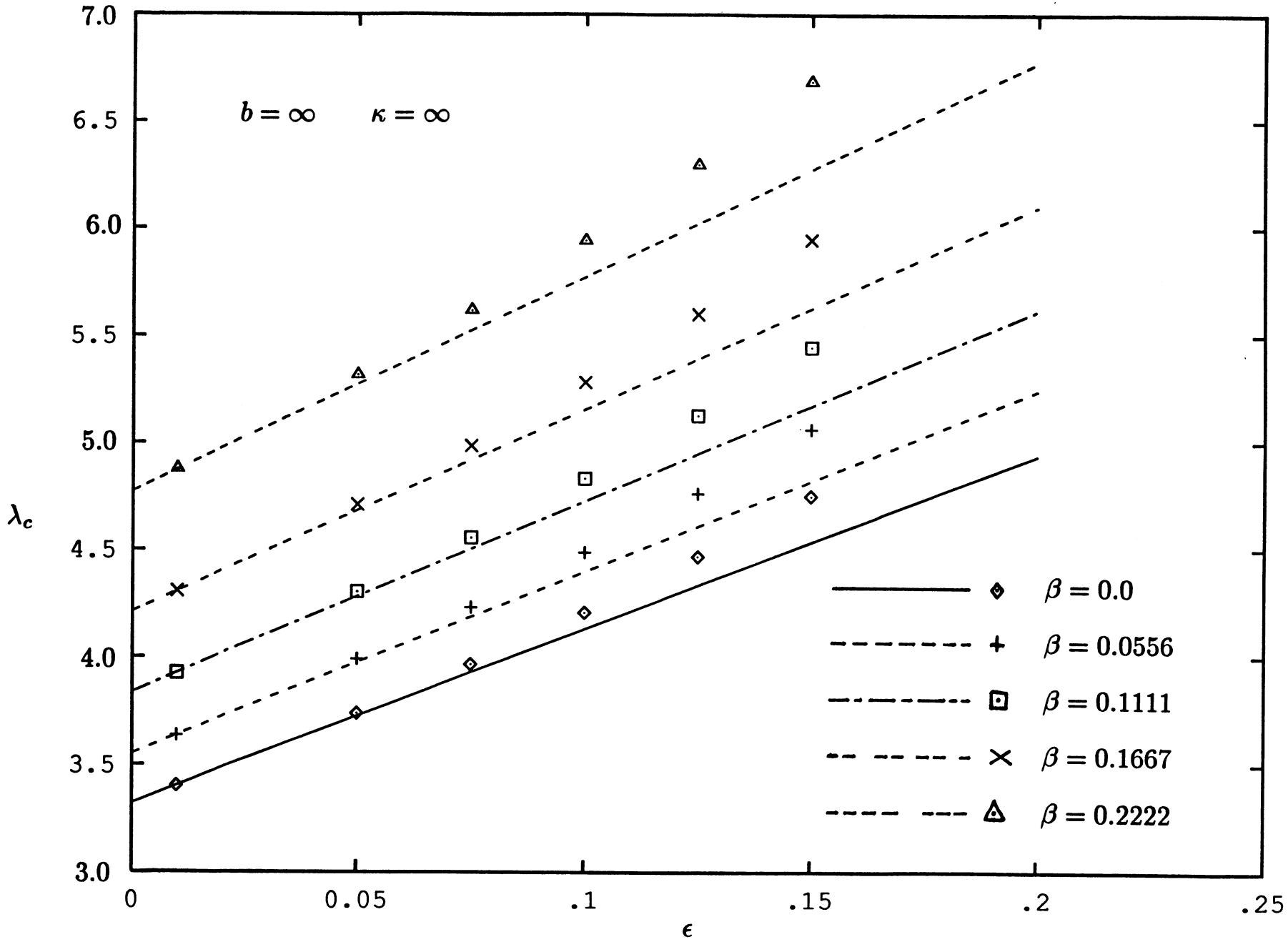
7.0
6.5
6.0
5.5
5.0
4.5
4.0
3.5
3.0
λ_c
$b = \infty$
$\kappa = \infty$
0
0.05
.1
.15
.2
.25
ϵ
$\beta = 0.0$
$\beta = 0.0556$
$\beta = 0.1111$
$\beta = 0.1667$
$\beta = 0.2222$

Figure 3

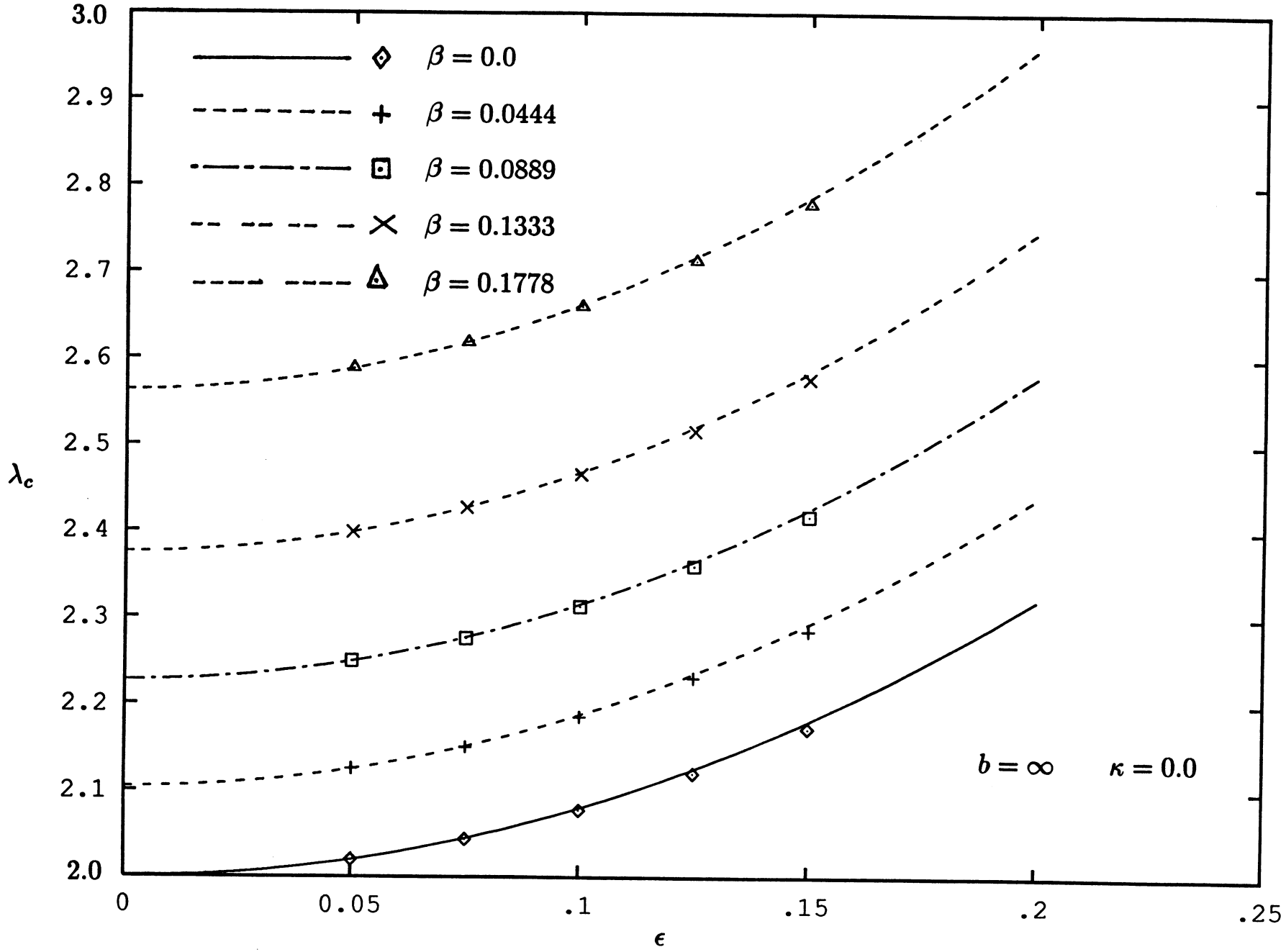
3.0
2.9
2.8
2.7
2.6
2.5
2.4
2.3
2.2
2.1
2.0
λ_c
0
0.05
.1
.15
.2
.25
ϵ
$\beta = 0.0$
$\beta = 0.0444$
$\beta = 0.0889$
$\beta = 0.1333$
$\beta = 0.1778$
$b = \infty$
$\kappa = 0.0$

Figure 4

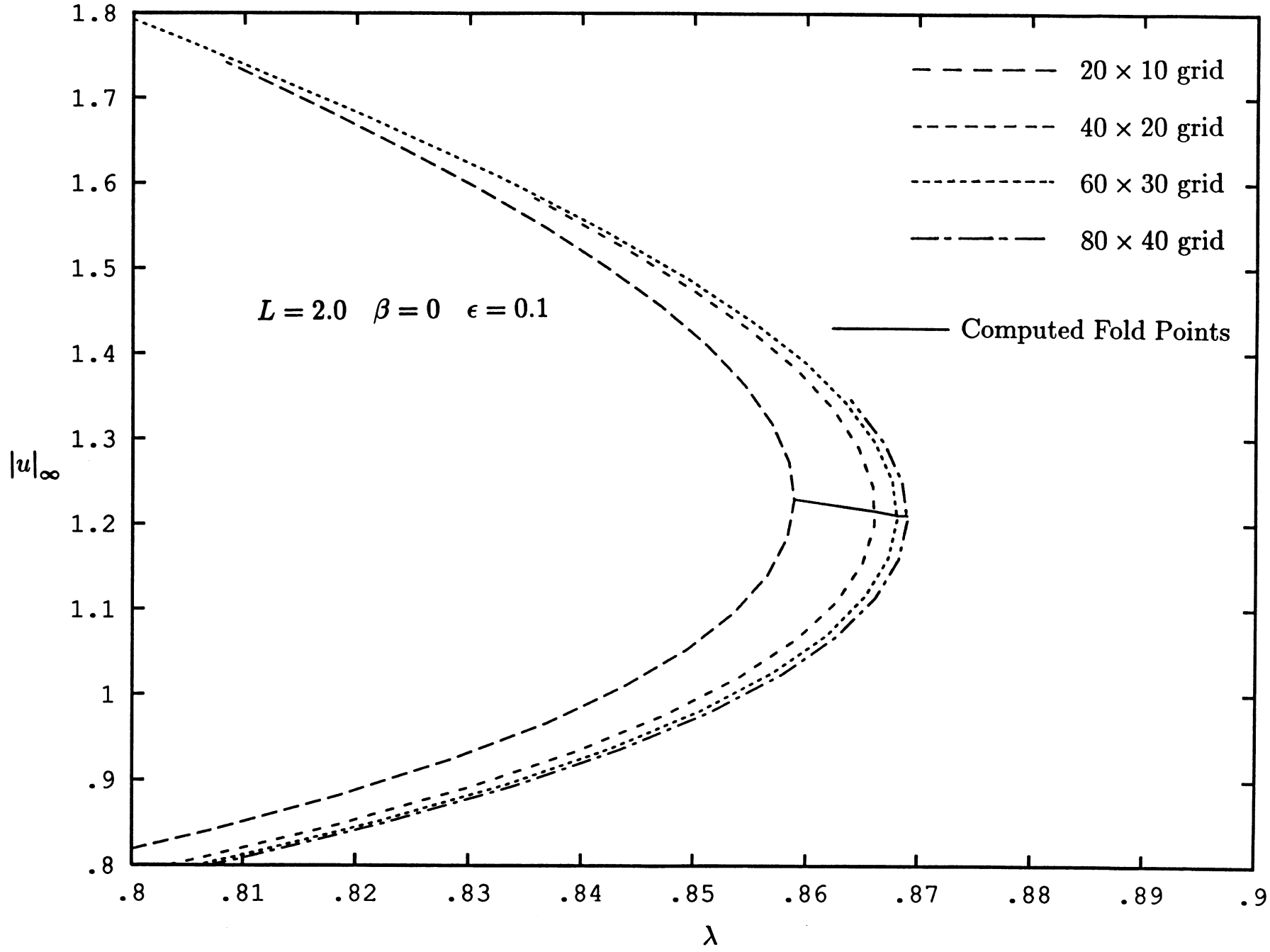
1.8
1.7
1.6
1.5
1.4
1.3
1.2
1.1
1
.9
.8
$|u|_\infty$
.8
.81
.82
.83
.84
.85
.86
.87
.88
.89
.9
λ
$L = 2.0 \quad \beta = 0 \quad \epsilon = 0.1$
20 × 10 grid
40 × 20 grid
60 × 30 grid
80 × 40 grid
Computed Fold Points

Figure 5

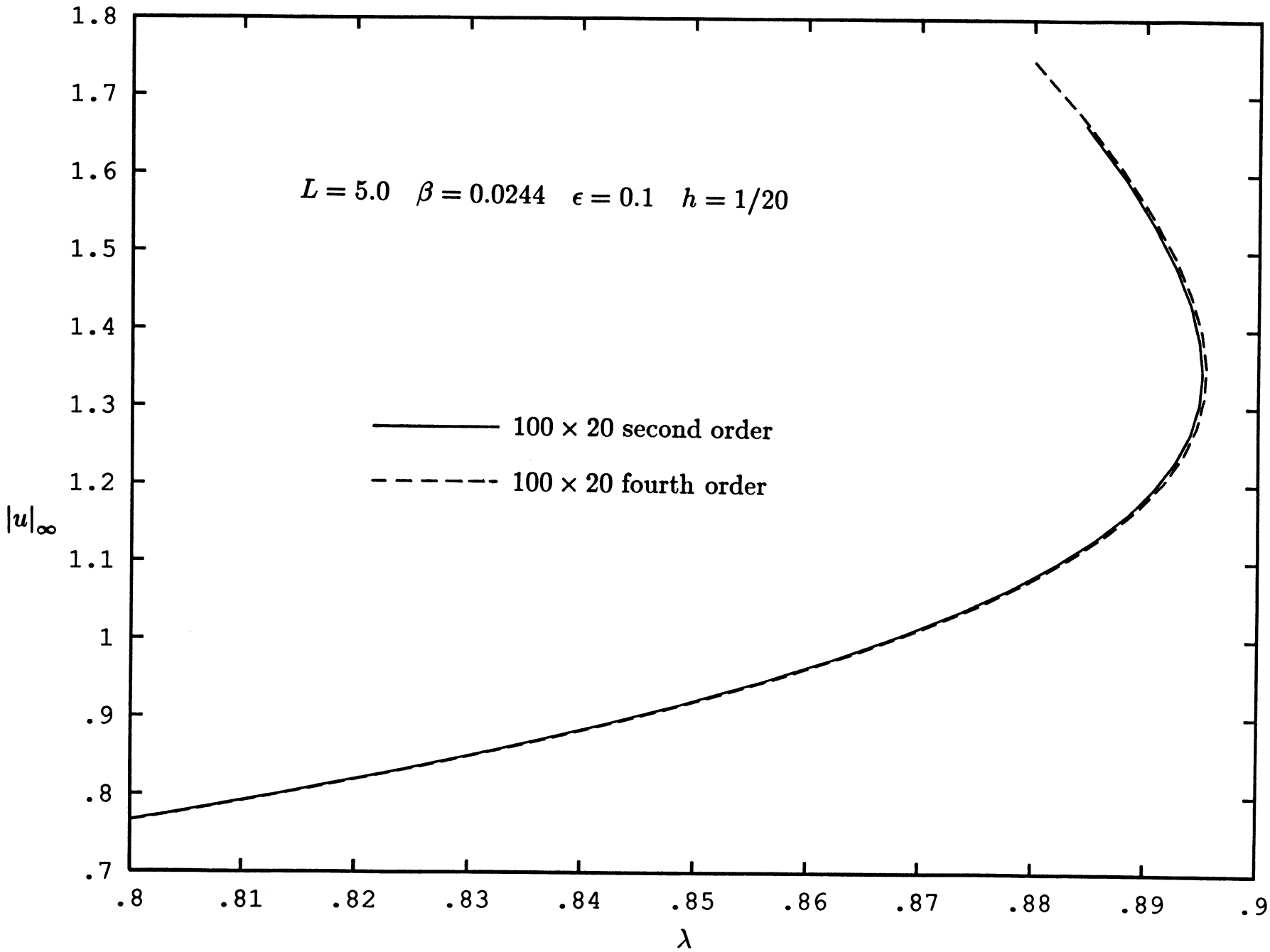
1.8
1.7
1.6
1.5
1.4
1.3
1.2
1.1
1
.9
.8
.7
$|u|_\infty$
$L = 5.0 \quad \beta = 0.0244 \quad \epsilon = 0.1 \quad h = 1/20$
100 × 20 second order
100 × 20 fourth order
.8
.81
.82
.83
.84
.85
.86
.87
.88
.89
.9
λ

Figure 6

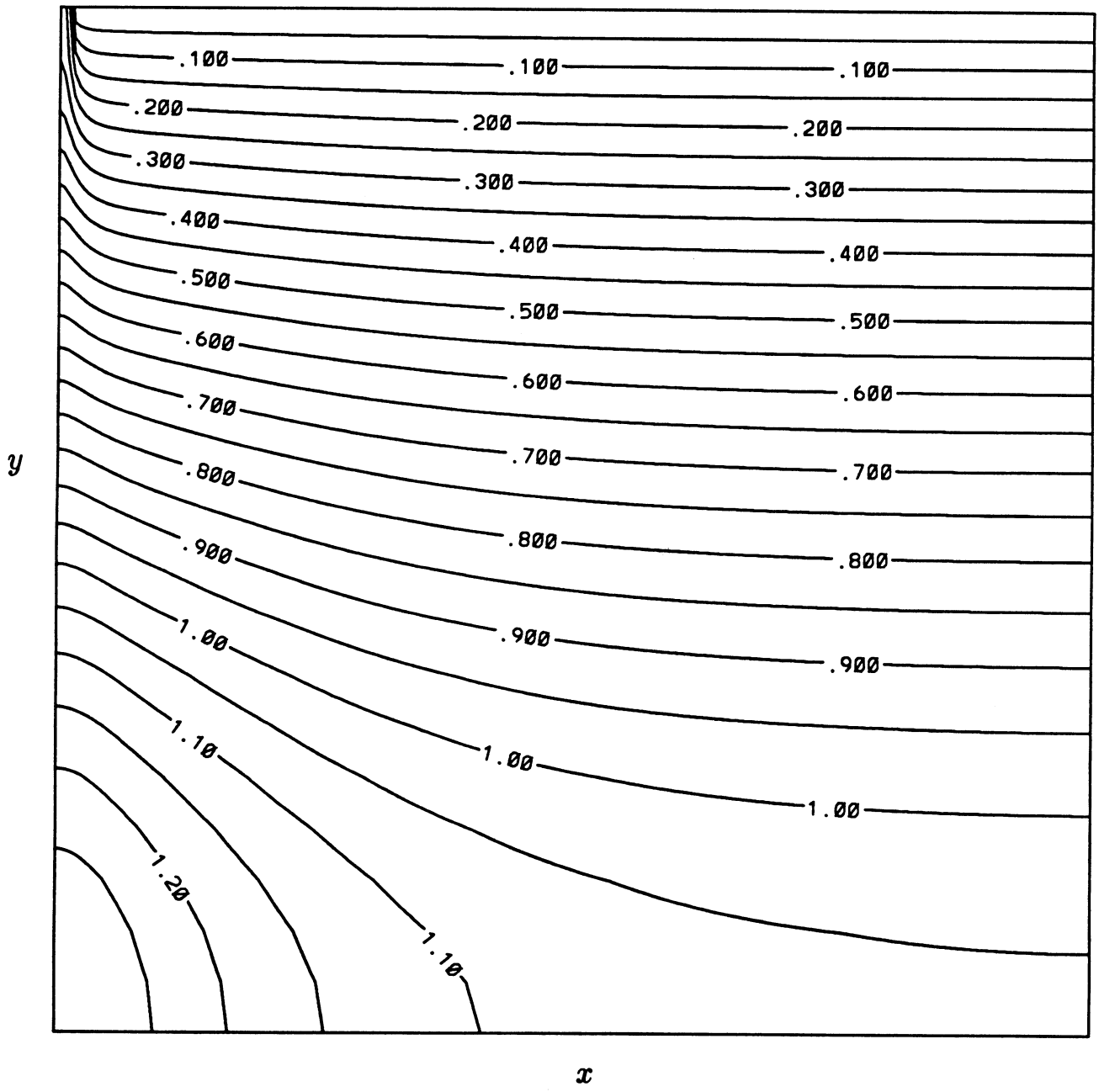
.100
.100
.100
.200
.200
.200
.300
.300
.300
.400
.400
.400
.500
.500
.500
.600
.600
.600
.700
.700
.700
.800
.800
.800
.900
.900
.900
1.00
1.00
1.00
1.10
1.10
1.20
y
x

Figure 7

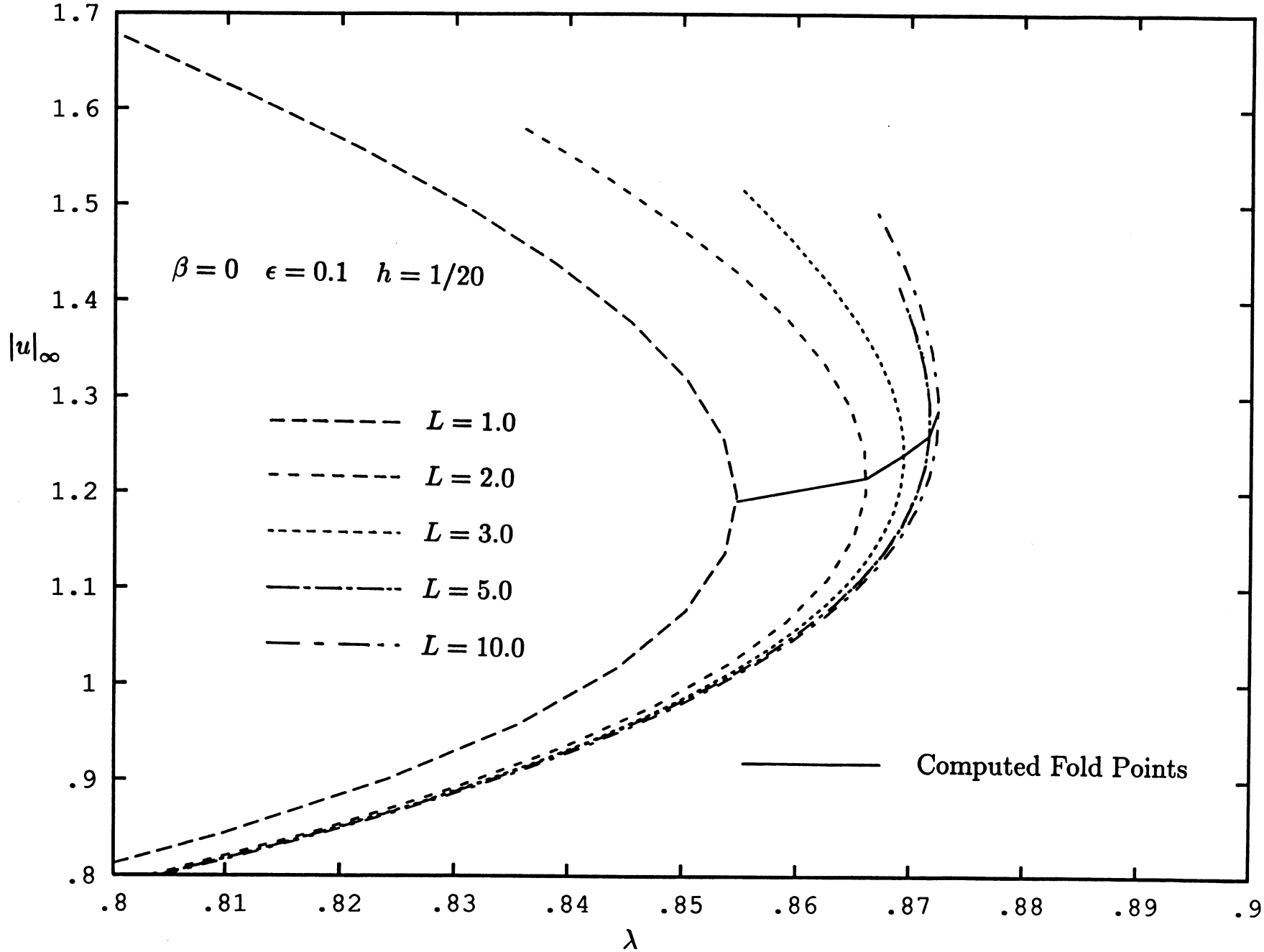
1.7
1.6
1.5
1.4
1.3
1.2
1.1
1
.9
.8
$|u|_\infty$
$\beta = 0 \quad \epsilon = 0.1 \quad h = 1/20$
$L = 1.0$
$L = 2.0$
$L = 3.0$
$L = 5.0$
$L = 10.0$
Computed Fold Points
.8
.81
.82
.83
.84
.85
.86
.87
.88
.89
.9
λ

Figure 8

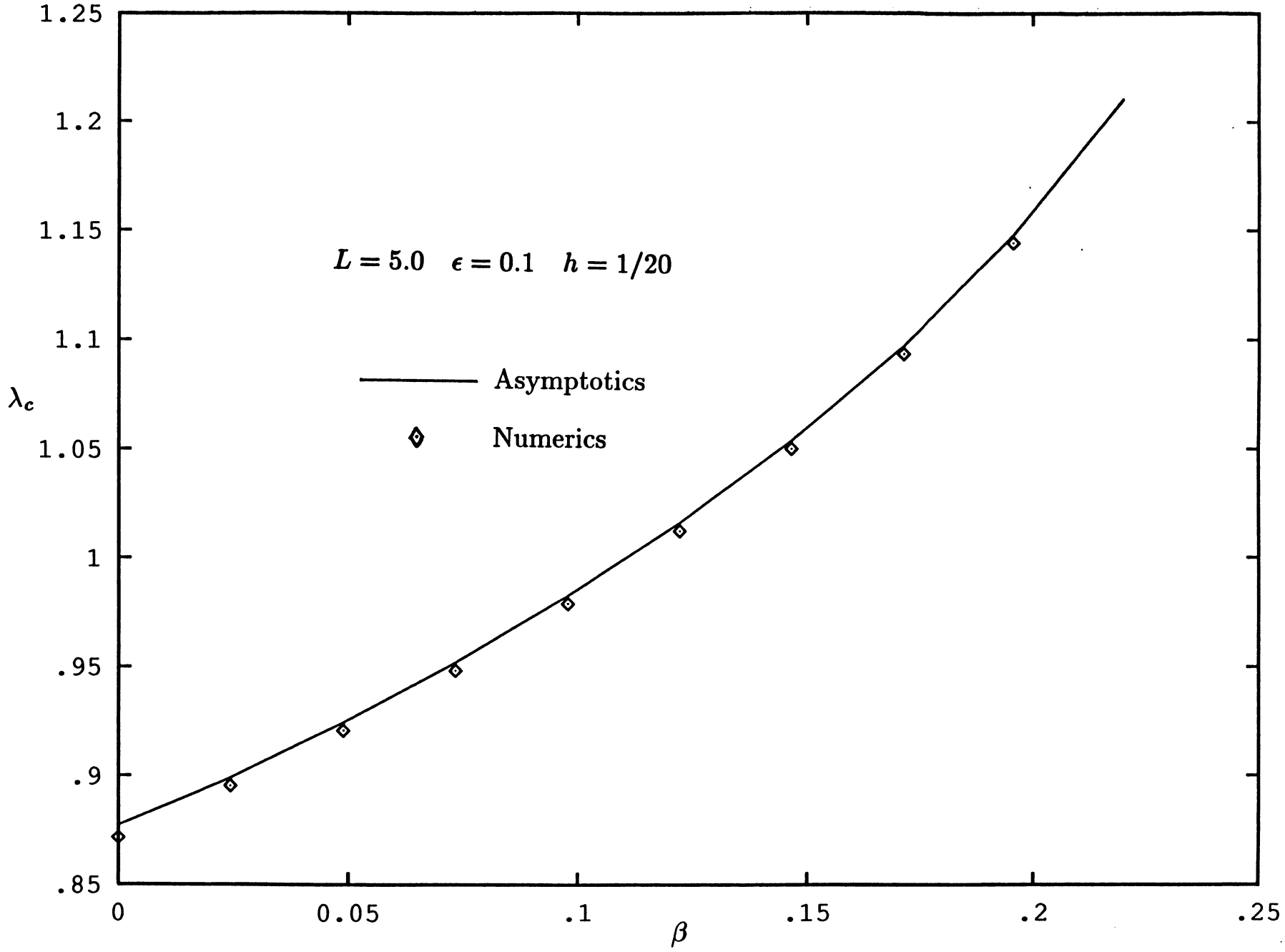
1.25
1.2
1.15
1.1
1.05
1
.95
.9
.85
λ_c
$L = 5.0 \quad \epsilon = 0.1 \quad h = 1/20$
Asymptotics
Numerics
0
0.05
.1
.15
.2
.25
β

Figure 9